ANTIOXIDANTS & REDOX SIGNALING
Volume 15, Number 9, 2011

DOI: 10.1089/ars.2010.3751

ORIGINAL RESEARCH COMMUNICATION

Activation of Akt Rescues Endoplasmic Reticulum Stress-Impaired Murine Cardiac Contractile Function *via* Glycogen Synthase Kinase-3β-Mediated Suppression of Mitochondrial Permeation Pore Opening

Yingmei Zhang,[1,2] Zhi Xia,[2] Karissa H. La Cour,[2] and Jun Ren[1,2]

Abstract

Aims: The present study was designed to examine the impact of chronic Akt activation on endoplasmic reticulum (ER) stress-induced cardiac mechanical anomalies, if any, and the underlying mechanism involved. ***Results:*** Wild-type and transgenic mice with cardiac-specific overexpression of the active mutant of Akt (Myr-Akt) were subjected to the ER stress inducer tunicamycin (1 or 3 mg/kg). ER stress led to compromised echocardiographic (elevated left ventricular end-systolic diameter and reduced fractional shortening) and cardiomyocyte contractile function, intracellular Ca^{2+} mishandling, and cell survival in wild-type mice associated with mitochondrial damage. *In vitro* ER stress induction in murine cardiomyocytes upregulated the ER stress proteins *Gadd*153, GRP78, and phospho-eIF2α, and promoted reactive oxygen species production, carbonyl formation, apoptosis, mitochondrial membrane potential loss, and mitochondrial permeation pore (mPTP) opening associated with overtly impaired cardiomyocyte contractile and intracellular Ca^{2+} properties. Interestingly, these anomalies were mitigated by chronic Akt activation or the ER chaperon tauroursodeoxycholic acid (TUDCA). Treatment with tunicamycin also dephosphorylated Akt and its downstream signal glycogen synthase kinase 3β (GSK3β) (leading to activation of GSK3β), the effect of which was abrogated by Akt activation and TUDCA. The ER stress-induced cardiomyocyte contractile and mitochondrial anomalies were obliterated by the mPTP inhibitor cyclosporin A, GSK3β inhibitor SB216763, and ER stress inhibitor TUDCA. ***Innovation:*** This research reported the direct relationship between ER stress and cardiomyocyte contractile and mitochondrial anomalies for the first time. ***Conclusion:*** Taken together, these data suggest that ER stress may compromise cardiac contractile and intracellular Ca^{2+} properties, possibly through the Akt/GSK3β-dependent impairment of mitochondrial integrity. *Antioxid. Redox Signal*. 15, 2407–2424.

Introduction

Endoplasmic reticulum (ER) is an extensive intracellular membranous network involved in Ca^{2+} storage, Ca^{2+} signaling, glycosylation, and trafficking of membrane and secretory proteins. Efficient functioning of the ER is crucial for cell function and survival. Perturbations of the ER homeostasis by energy deprivation, infection, increased protein trafficking, expression of mutant proteins incompatible for folding, and chemical triggers such as tunicamycin interfere with the proper functioning of ER to create a condition namely ER stress (14, 25, 26, 33, 39). Although ER stress represents a defense mechanism against external insult, excessive ER stress may ultimately trigger pathological responses through the activation of a complex signaling network called unfolded protein response (UPR) (25, 26, 29, 33, 39). Three classes of ER stress transducers have been identified, including inositol-requiring protein-1 (IRE1), the protein kinase RNA (PKR)-like ER kinase (PERK)-translation initiation factor eIF-2α pathway, and transcription factor-6 (ATF6) (9, 39). ER stress has been implicated to participate in a wide array of diseases such as obesity, diabetes, neurodegenerative disorders, alcoholism, hypertrophic, and ischemia reperfusion

Innovation

This research reported the direct relationship between endoplasmic reticulum stress and cardiomyocyte contractile and mitochondrial anomalies for the first time.

[1]Department of Cardiology, Xijing Hospital, Fourth Military Medical University, Xi'an, China.
[2]Center for Cardiovascular Research and Alternative Medicine, University of Wyoming College of Health Sciences, Laramie, Wyoming.

heart diseases (9, 17, 24, 26, 29, 31, 32). Consequently, a number of pharmacological compounds capable of alleviating ER stress through their chemical chaperon properties such as tauroursodeoxycholic acid (TUDCA) are found beneficial in insulin resistance and cardiovascular diseases (2, 26, 29, 33). However, the precise mechanisms underscoring ER stress-induced cardiovascular anomalies have not been elucidated, making it somewhat difficult to develop chaperon and other therapeutic intervention against ER stress-induced pathology. Recent evidence from our lab as well as others has unveiled a rather complex interplay between ER stress and oxidative stress in cardiac pathologies. In particular, ER stress seems to serve as the cause and consequence for production of reactive oxygen species (ROS) and redox deviation (11, 23, 33). Given that ER stress is closely associated with the reduced phosphorylation of Akt, an essential cardiac survival factor, and its downstream signal glycogen synthase kinase 3β (GSK3β) in the heart (18), this study was designed to test the hypothesis that ER stress may compromise cardiac function through an Akt-dependent cellular mechanism, whereas restored Akt activation in the heart may protect against ER stress-induced cardiac pathological changes. To this end, the effect of cardiac-specific overexpression of the active mutant of Akt on ER stress-induced cardiac contractile and intracellular Ca^{2+} defects, if any, was evaluated both *in vitro* and *in vivo*. To better elucidate the interplay between ER stress and oxidative stress in ER stress-induced cardiac responses, ROS production, protein damage, apoptosis, mitochondrial integrity including mitochondrial membrane potential and mitochondrial permeation pore (mPTP) opening, as well as cell signaling of Akt and GSK3β were scrutinized in wild-type (WT) and transgenic mice with intrinsic Akt activation after ER stress induction. Levels of caspase-8 and pro-caspase-9 were assessed to evaluate the role of receptor and mitochondrial death domains, respectively (15). In addition, expression of caspase-12, an ER-specific member of the caspase family to mediate ER-specific apoptosis (28), was also monitored under ER stress and chronic Akt activation.

Results

Effect of ER stress on echocardiographic, cardiomyocyte contractile, and intracellular Ca^{2+} properties in mice

To examine the impact of ER stress and Akt activation on cardiac contractile function *in vivo*, WT and MyAkt mice were challenged with tunicamycin (1 or 3 mg/kg, i.p.) for 48 h (35, 45) before assessment of echocardiographic and cardiomyocyte mechanical properties. Our data depicted that tunicamycin significantly decreased fractional shortening, peak shortening (PS), and maximal velocity of shortening/relengthening ($\pm$dL/dt); increased left ventricular end-systolic diameter (LVESD); and prolonged relengthening duration (TR_{90}) without affecting left ventricular end-diastolic diameter (LVEDD) and duration of shortening (time-to-peak shortening [TPS]). The mechanical responses elicited by both dosages of tunicamycin were comparable. While Akt activation itself did not elicit any overt effect on the mechanical parameters tested, it mitigated ER stress (at both tunicamycin dosages)-induced alterations in fractional shortening, PS, $\pm$ dL/dt, LVESD, and TR_{90} without affecting LVEDD and TPS (Fig. 1). To explore the possible mechanisms of action behind Akt activation-elicited beneficial effect against ER stress, intracellular Ca^{2+} handling was evaluated using fura-2 fluorescence dye. Our data demonstrated in Figure 2 revealed that ER stress induction significantly increased resting intracellular Ca^{2+} levels, decreased electrically stimulated rise in intracellular Ca^{2+}, as well as slowed intracellular Ca^{2+} clearance rate (single or biexponential). Both dosages of tunicamycin elicited comparable changes in intracellular Ca^{2+} properties although resting intracellular Ca^{2+} level was only overtly elevated by the higher dose of tunicamycin. Therefore, tunicamycin at 3 mg/kg was used for the remaining of our study to induce ER stress *in vivo*. Although Akt activation itself failed to exert any notable effect on intracellular Ca^{2+} properties, it nullified both dosages of tunicamycin-induced intracellular Ca^{2+} mishandling. In addition, thapsigargin, an inhibitor of ER-specific Ca^{2+}-ATPase, elicited cardiac contractile and intracellular Ca^{2+} anomalies both *in vivo* and *in vitro* in a manner reminiscent of tunicamycin (data not shown), consolidating cardiac responses under ER stress.

ER stress, cell survival, mitochondrial function, and Akt/GSK3β phosphorylation in WT and MyAkt mice challenged with tunicamycin in vivo

Western blot analysis confirmed the presence of ER stress with upregulated *Gadd*153 and GRP78 in myocardium after tunicamycin treatment (3 mg/kg). ER stress induction reduced cell survival rate and promoted mitochondrial damage as assessed by MTT and aconitase activity, respectively. Although Akt activation itself did not exert any notable effect on ER stress, cell survival, and mitochondrial integrity, it obliterated tunicamycin-induced change in cell survival and mitochondrial integrity without affecting the ER stress status. Coadministration of the ER stress inhibitor TUDCA [50 mg/kg (2)] with tunicamycin rescued against tunicamycin-induced ER stress, loss of cell survival, and mitochondrial integrity *in vivo*. Phosphorylation of Akt and its downstream signaling molecule GSK3β was significantly dampened after *in vivo* ER stress induction in mice, the effect of which was overridden by chronic Akt activation and coadministration of the ER chaperon TUDCA (Fig. 3).

Effect of in vitro *ER stress on cardiomyocyte contractile and intracellular Ca^{2+} properties*

We further tested the effect of ER stress on cardiomyocyte function *in vitro*. Neither ER stress induction nor Akt activation significantly affected resting cell length. Similar to its effects *in vivo*, tunicamycin (3 μg/ml) significantly decreased PS amplitude and maximal velocity of shortening/relengthening ($\pm$dL/dt) as well as prolonged relengthening duration (TR_{90}) without affecting TPS. While Akt activation itself did not elicit any effect on the mechanical parameters tested, it mitigated ER stress-induced alterations in PS, $\pm$ dL/dt, and TR_{90} without affecting TPS. Not surprisingly, the ER stress inhibitor TUDCA (500 μM) abolished tunicamycin-elicited cardiomyocyte contractile dysfunction without eliciting any overt effect by itself (Fig. 4). Our data shown in Figure 5 exhibited that ER stress induction significantly increased resting intracellular Ca^{2+} levels, decreased electrically stimulated rise in intracellular Ca^{2+}, as well as slowed down intracellular Ca^{2+} clearance rate (single or biexponential). Although Akt activation and ER stress inhibition with

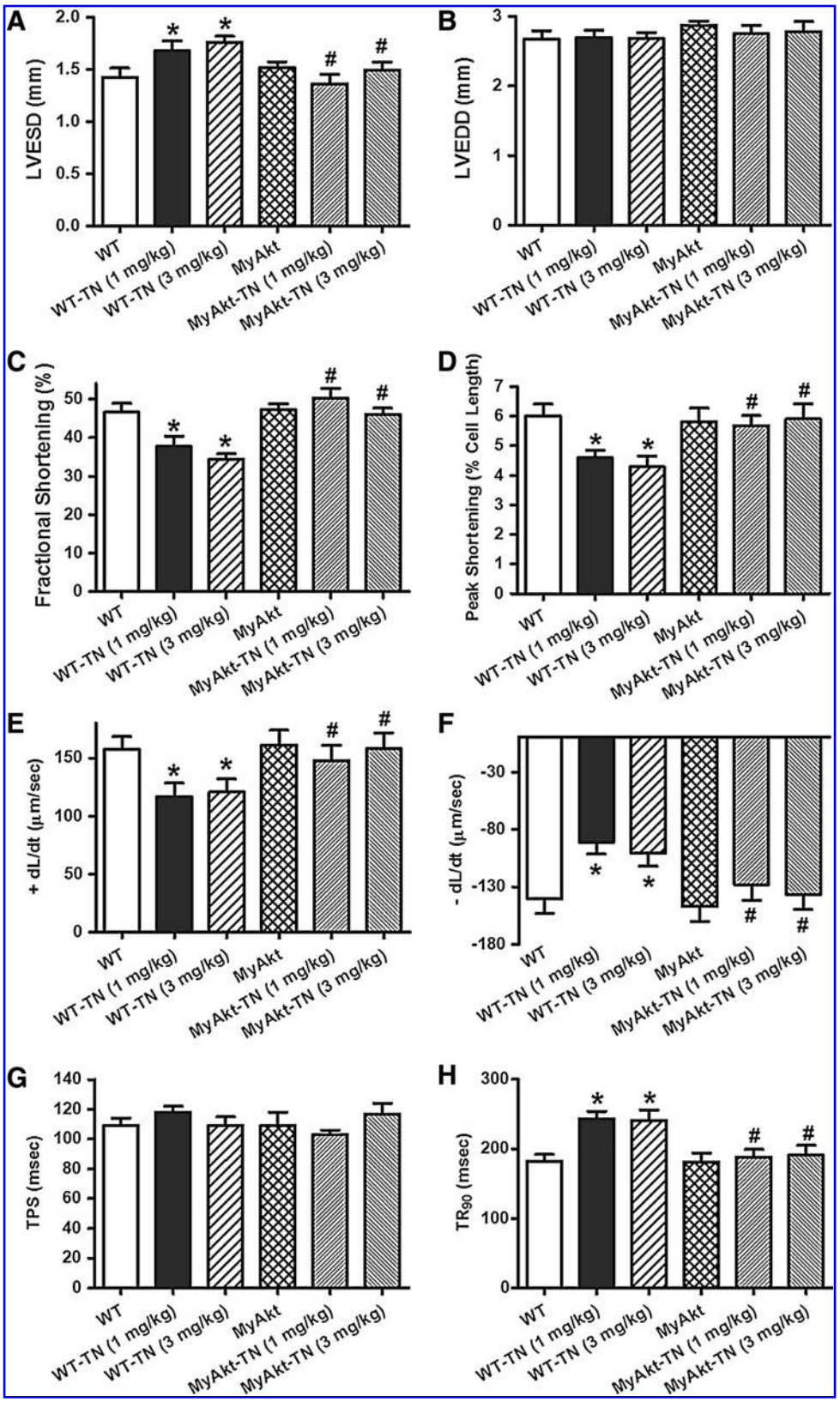

FIG. 1. Effect of *in vivo* tunicamycin (TN) challenge (1 or 3 mg/kg, i.p. for 48 h) on echocardiographic and cardiomyocyte contractile properties from wild-type (WT) and MyAkt mice. (A) Left ventricular end-systolic diameter (LVESD) using echocardiography; **(B)** left ventricular end-diastolic diameter (LVEDD) using echocardiography; **(C)** fractional shortening using echocardiography; **(D)** peak shortening (PS) (% of cell length) in cardiomyocytes; **(E)** maximal velocity of shortening (+dL/dt); **(F)** maximal velocity of relengthening (−dL/dt); **(G)** time-to-peak shortening (TPS); and **(H)** time-to-90% relengthening (TR_{90}). Mean ± SEM, $n = 6$–7 mice and 86–87 cells for *panels* **(A–C)** and *panels* **(D–H)**, respectively, $^{*}p < 0.05$ *versus* WT group; $^{\#}p < 0.05$ *versus* respective WT-TN group.

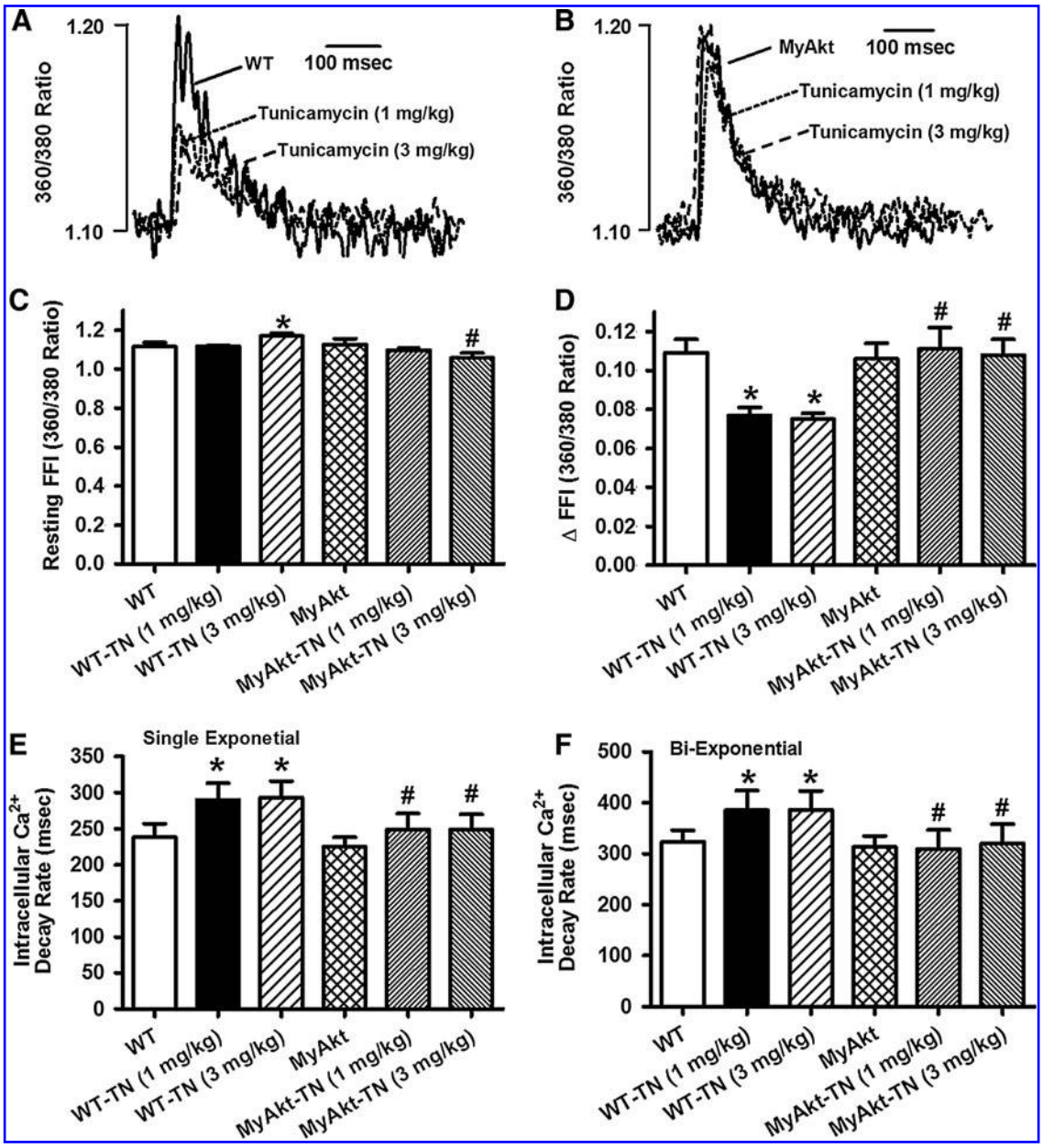

FIG. 2. Effect of *in vivo* TN challenge (1 or 3 mg/kg, i.p. for 48 h) on intracellular Ca^{2+} properties in cardiomyocytes from WT and MyAkt mice. (A) Representative intracellular Ca^{2+} transients in cardiomyocytes from WT mice with or without TN; **(B)** representative intracellular Ca^{2+} transients in cardiomyocytes from MyAkt mice with or without TN; **(C)** resting fura-2 fluorescence intensity (FFI); **(D)** electrically stimulated increase in FFI (ΔFFI); **(E)** intracellular Ca^{2+} decay rate (single exponential); and **(F)** intracellular Ca^{2+} decay rate (biexponential). Mean ± SEM, $n = 60$ cells per group, $^{*}p < 0.05$ *versus* WT group; $^{\#}p < 0.05$ *versus* respective WT-TN group.

TUDCA failed to exert any notable effect on intracellular Ca^{2+} properties, they independently nullified the ER stress-induced abnormalities in intracellular Ca^{2+} handling.

Effect of Akt activation and TUDCA on in vitro *tunicamycin-induced ER stress*

To confirm the presence of ER stress after *in vitro* tunicamycin treatment, the ER stress markers *Gadd*153, GRP78, and phospho-eIF2α (peIF2α) were evaluated. Our data depicted overt increase in the levels of *Gadd*153, GRP78, and peIF2α after tunicamycin treatment (3 μg/ml), the effect of which was abolished by the ER stress inhibitor TUDCA (500 μM) but was unaffected by chronic Akt activation. Akt activation or TUDCA itself failed to alter the protein expression of *Gadd*153, GRP78, and peIF2α (Fig. 6). Expression of pan eIF2α was unaffected by ER stress induction, Akt activation, or TUDCA (data not shown).

Effect of Akt activation on ER stress-induced ROS production, cell death, and protein damage

Given that ER stress is known to elicit myocardial damage through accumulation of ROS and cell death (11), the effect of

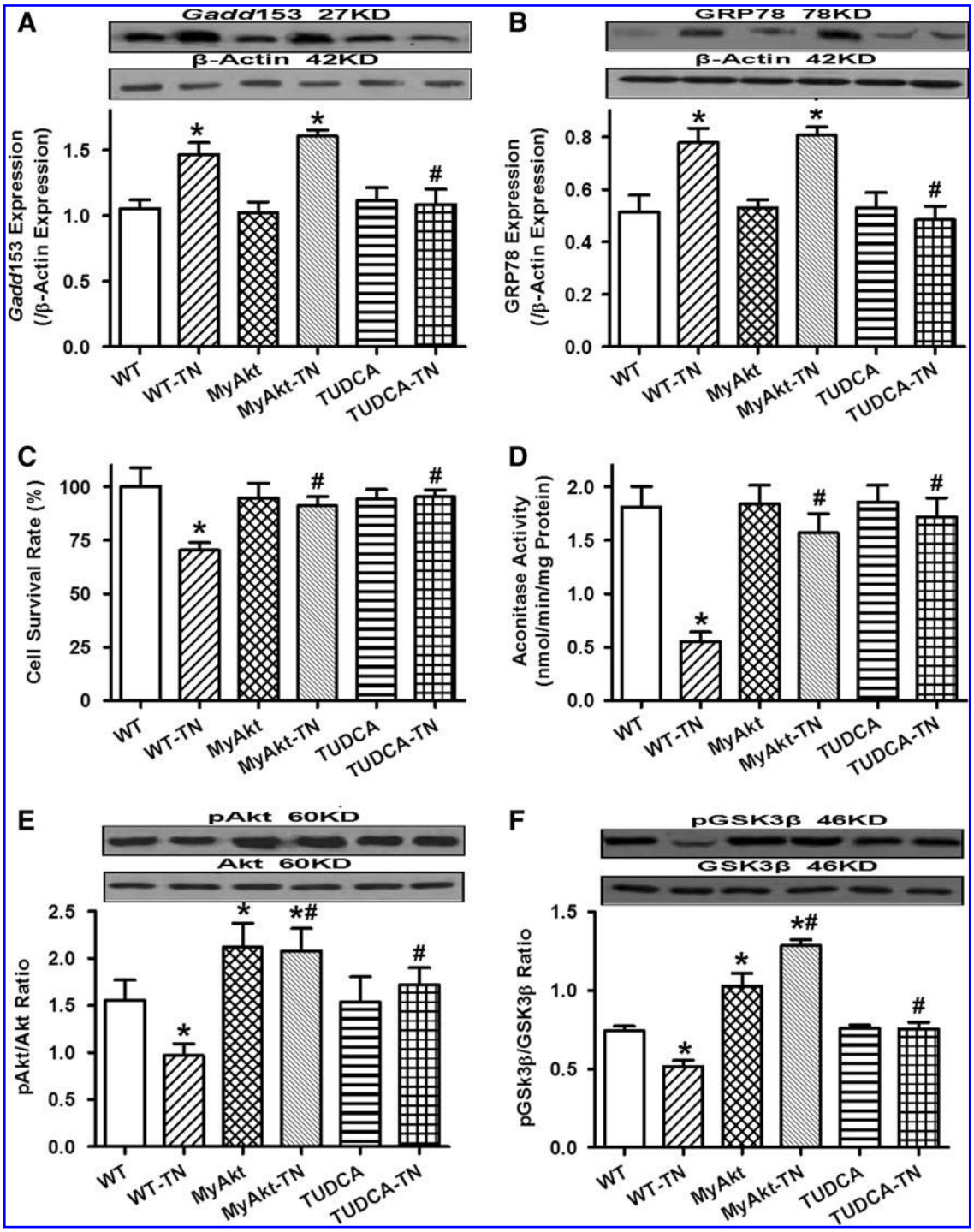

FIG. 3. Effect of *in vivo* TN challenge (3 mg/kg, i.p. for 48 h) on endoplasmic reticulum (ER) stress, cell survival, mitochondrial integrity (aconitase activity), and phosphorylation of Akt and glycogen synthase kinase 3β (GSK3β) in WT and MyAkt mice. A cohort of WT mice were injected with the ER stress inhibitor tauroursodeoxycholic acid (TUDCA) (50 mg/kg, i.p.) at the time of TN challenge. **(A)** *Gadd*153 expression; **(B)** GRP78 expression; **(C)** cell survival; **(D)** aconitase activity; **(E)** pAkt-to-Akt ratio; and **(F)** pGSK3*β*-to-GSK3*β* ratio. *Insets*: Representative gel blots depicting the ER stress proteins *Gadd*153 and GRP78, as well as pan and phosphorylated Akt and GSK3*β* using specific antibodies (*β*-actin was used as the loading control). All protein expressions were normalized to that of *β*-actin. Mean ± SEM, $n = 5$–7 hearts per group, $^{*}p < 0.05$ *versus* WT group, $^{\#}p < 0.05$ *versus* WT-TN group.

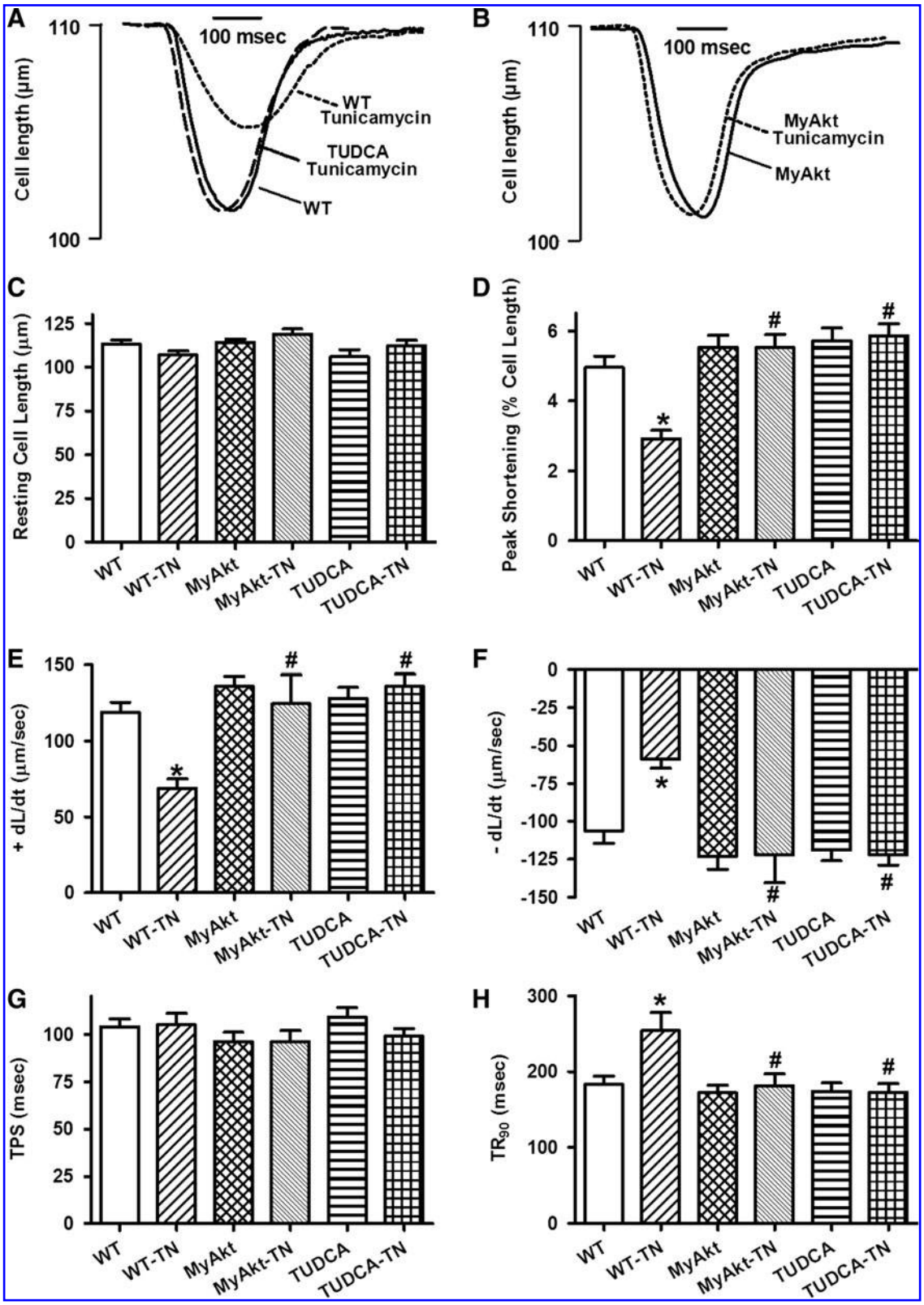

FIG. 4. Effect of TN on cell shortening in isolated cardiomyocytes from WT and MyAkt mice. Murine cardiomyocytes were incubated with TN (3 μg/ml) for 5–6 h *in vitro* before assessment of mechanical properties. A cohort of WT cardiomyocytes were coincubated with the ER stress inhibitor TUDCA (500 μM) alone with TN. **(A)** Representative contractile traces in cardiomyocytes from WT mice in the absence or presence of TN or TUDCA; **(B)** representative contractile traces in cardiomyocytes from MyAkt mice in the absence or presence of TN; **(C)** resting cell length; **(D)** PS (% of resting cell length); **(E)** maximal velocity of shortening (+dL/dt); **(F)** maximal velocity of relengthening (−dL/dt); **(G)** TPS; and **(H)** time-to-90% relengthening (TR_{90}). Mean ± SEM, $n = 80$ cells per group, $^{*}p < 0.05$ *versus* WT group; $^{\#}p < 0.05$ *versus* WT-TN group.

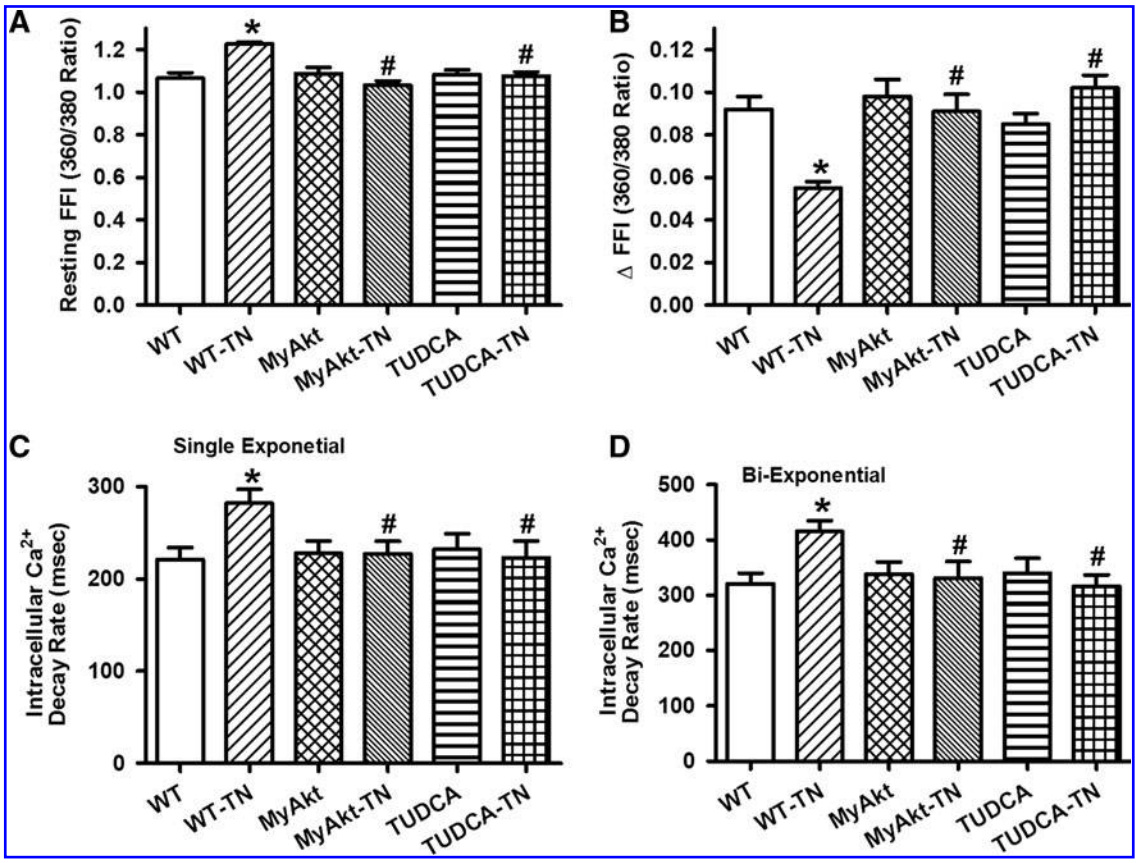

FIG. 5. Effect of TN on intracellular Ca^{2+} properties in cardiomyocytes from WT and MyAkt mice. Murine cardiomyocytes were incubated with TN (3 μg/ml) for 5–6 h *in vitro* before intracellular Ca^{2+} evaluation. **(A)** Baseline FFI; **(B)** electrically stimulated increase in FFI (ΔFFI); **(C)** intracellular Ca^{2+} decay rate (single exponential); and **(D)** intracellular Ca^{2+} decay rate (biexponential). Mean ± SEM, $n = 52$–54 cells per group, $^{*}p < 0.05$ *versus* WT group; $^{\#}p < 0.05$ *versus* WT-TN group.

Akt activation on *in vitro* ER stress-induced ROS production, protein damage, and cell death was examined. Using the intracellular fluoroprobe CM-H_2DCFDA, data shown in Figure 7 depicted elevated ROS generation and cell death after tunicamycin challenge, the effects of which were significantly attenuated or mitigated by Akt activation, TUDCA, or the mPTP inhibitor cyclosporin A (200 n*M*). Moreover, the antioxidant catalase-polyethylene glycol (catalase-PEG, 15,000 IU/ml) effectively nullified H_2O_2 (100 μM)-induced ROS accumulation. Further scrutiny of the level and distribution of protein carbonyl depicted that tunicamycin significantly increased protein carbonyl levels both *in vitro* and *in vivo*. Although TUDCA or Akt activation did not elicit any effect on protein carbonyl levels by itself, they were able to significantly alleviated or abrogated ER stress-induced protein damage (Fig. 8A, B). In addition, ER stress induction by tunicamycin *in vitro* overtly promoted apoptosis as evidenced by caspase-3 assay. Level of the mitochondrial death protein pro-caspase-9 and the ER stress-specific apoptotic protein caspase-12 (but not the death receptor apoptotic protein caspase-8) were significantly upregulated by tunicamycin. While Akt activation and TUDCA did not exert any notable effect on apoptosis themselves, they independently nullified ER stress-induced increases in caspase-3 activity and Pro-caspase-9 level without affecting the levels of caspase-8 and cleaved caspase-12 (Fig. 8C–F).

Effect of Akt activation on in vitro *ER stress-induced change of mitochondrial function*

To further examine the role of mitochondria in Akt activation-offered protection against ER stress-induced ROS production, protein damage, cell death, and mechanical dysfunction, mitochondrial membrane potential and mPTP opening were measured using the JC-1 fluorescent probe and NAD^+, respectively. Our results revealed a significant loss of mitochondrial membrane potential and NAD^+ content in cardiomyocytes after tunicamycin treatment. Consistent with their effects on ROS production, protein damage, cell survival, and mechanical properties, Akt activation and ER chaperon TUDCA (500 μM) (11) significantly attenuated or ablated ER stress-elicited damage to mitochondrial integrity as evidenced by restored mitochondrial membrane potential and NAD^+ content. Akt activation and TUDCA themselves did not exhibit any effect on mitochondrial membrane potential and NAD^+ content. To further evaluate the role of mPTP opening and GSK3β in ER stress-induced mitochondrial damage, cardiomyocytes from WT mice were treated with tunicamycin (3 μg/ml) for 5–6 h in the absence or presence of the mPTP inhibitor cyclosporin A (200 n*M*) (41) or the GSK3β inhibitor SB216763 (10 μM) (13) before the assessment of mitochondrial function. Intriguingly, both cyclosporin A and SB216763 were capable of preventing tunicamycin-induced loss of

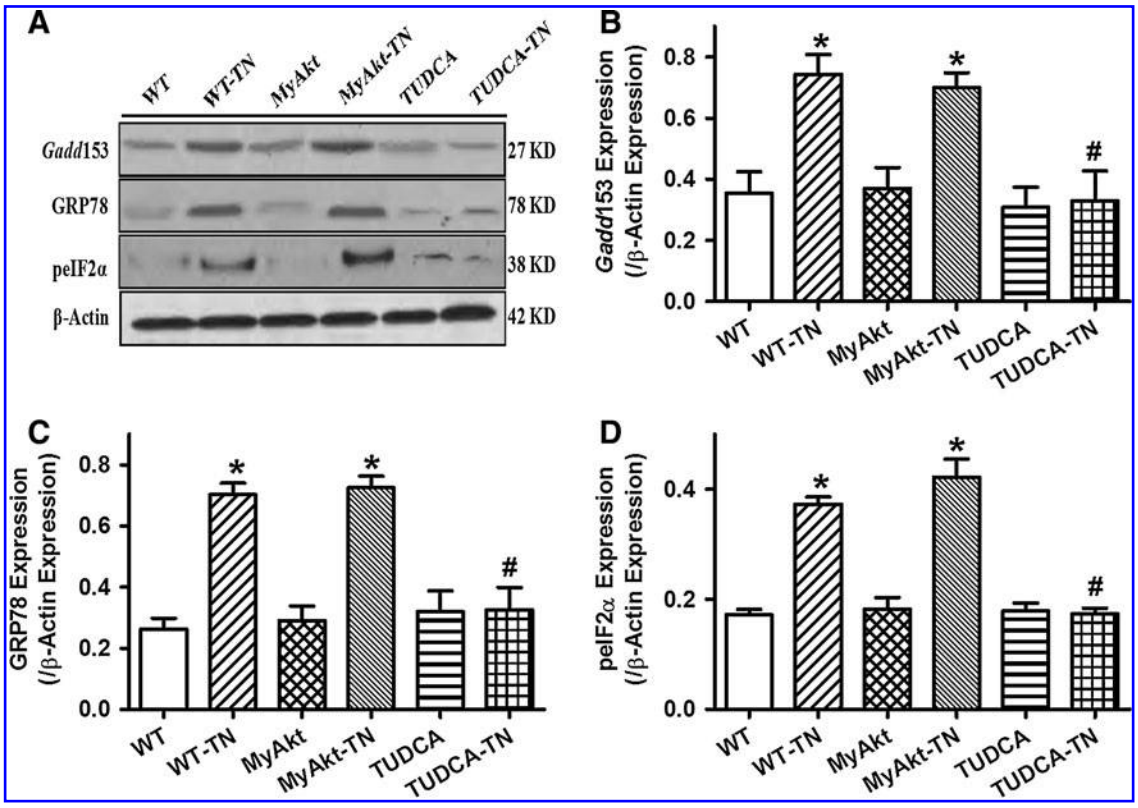

FIG. 6. Effect of TN on ER stress in cardiomyocytes from WT and MyAkt mice. Freshly isolated murine cardiomyocytes were incubated with TN (3 μg/ml) for 5–6 h *in vitro* before assessment of ER stress. A cohort of WT cardiomyocytes were coincubated with the ER stress inhibitor TUDCA (500 μM) alone with TN. **(A)** Representative gel blots depicting the ER stress proteins *Gadd*153, GRP78, and peIF2α using specific antibodies (β-actin was used as the loading control); **(B)** *Gadd*153 expression; **(C)** GRP78 expression; and **(D)** peIF2α expression. All protein expression was normalized to that of β-actin. Mean ± SEM, $n = 5$–7 isolations per group, $^{*}p < 0.05$ *versus* WT group; $^{\#}p < 0.05$ *versus* WT-TN group.

mitochondrial membrane potential and NAD^+ content without eliciting any discernable effect themselves (Fig. 9).

Effect of Akt activation on in vitro *ER stress-induced change in expression of Akt and GSK3*β

To further elucidate the potential signaling mechanisms involved in Akt activation-induced protection against cardiac ER stress, Western blot analysis was performed on Akt signaling and its downstream signaling molecule GSK3β. Similar to the *in vivo* findings, cardiomyocytes from MyAkt mice displayed significantly elevated levels of Akt and phosphorylated Akt (pAkt) (absolute value or the pAkt-to-Akt ratio) compared with those cells from WT mice. Similarly, cardiomyocytes from MyAkt mice displayed significantly elevated GSK3β phosphorylation (absolute value or the phosphorylated GSK3β [pGSK3β]-to-GSK3β ratio) compared with those cells from WT mice. Induction of ER stress by tunicamycin *in vitro* significantly inhibited the phosphorylation of Akt and GSK3β (absolute value or phosphorylated-to-pan protein ratio) without affecting the pan protein expression. Interestingly, the ER stress-triggered loss in phosphorylation of Akt and GSK3β was obliterated in cardiomyocytes from MyAkt mice (Supplementary Materials and Methods; Supplementary Data are available online at www.liebertonline.com/ars). Neither ER stress nor Akt activation altered the expression of pan GSK3β (Supplementary Fig. S1).

*Effects of inhibition of mPTP and GSK3*β *on ER stress-induced cardiomyocyte dysfunction*

To further evaluate the role of GSK3β and mPTP opening in ER stress-induced cardiac contractile dysfunction, murine cardiomyocytes from WT mice were treated with tunicamycin (3 μg/ml) for 5–6 h in the absence or presence of the mPTP inhibitor cyclosporine A (200 nM) (41) or the GSK3β inhibitor SB216763 (10 μM) (13) before assessment of cardiomyocyte mechanical function. The ER stress chaperon TUDCA (500 μM) was used as a positive control (11). While these pharmacological inhibitors failed to elicit any notable effect on cardiomyocyte mechanical parameters themselves, they independently nullified the tunicamycin-induced cardiomyocyte contractile dysfunctions including reduced PS amplitude and ± dL/dt as well as prolonged TR_{90}. Neither the resting cell length nor TPS was affected by tunicamycin or the pharmacological inhibitors (Fig. 10). These findings strongly favor a tie among GSK3β signaling, mitochondrial integrity, and cardiomyocyte mechanical function in ER stress.

Discussion

The salient findings of our study revealed that ER stress impairs echocardiographic, cardiomyocyte contractile function, intracellular Ca^{2+} homeostasis, and cell survival associated with ROS accumulation, protein carbonyl formation,

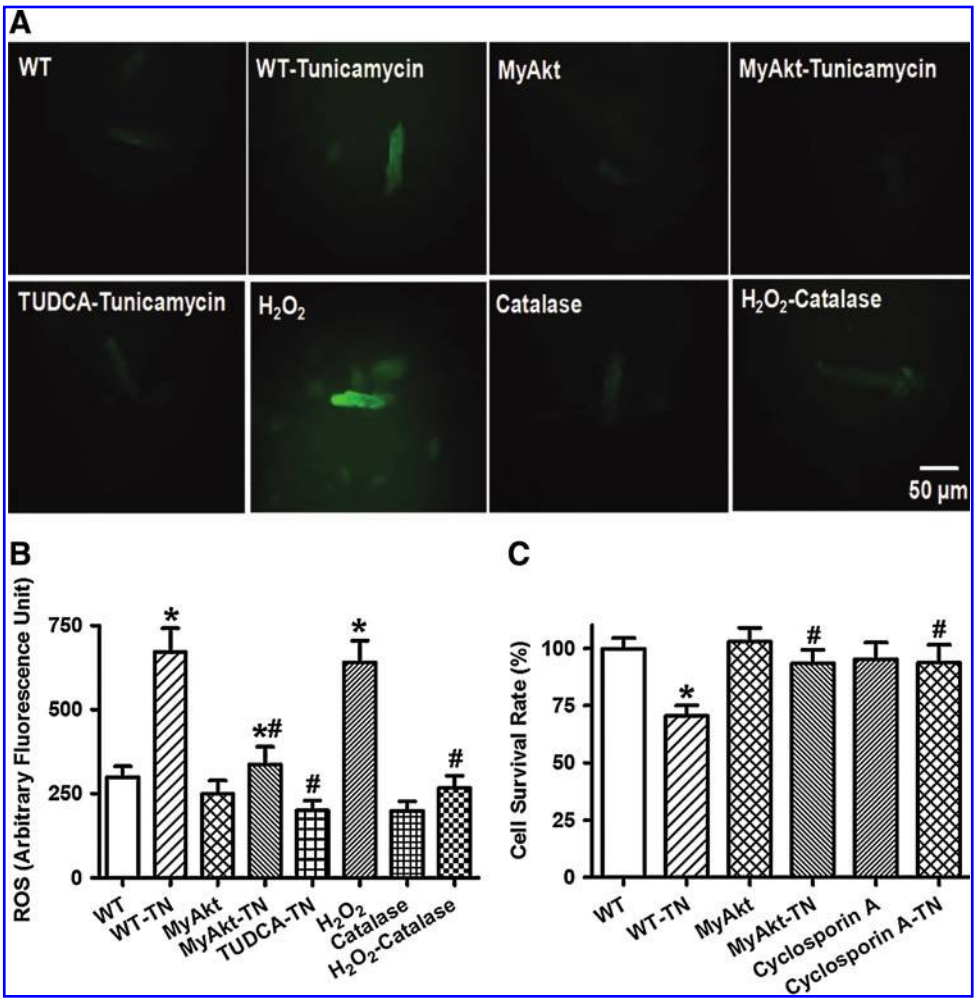

FIG. 7. Effect of TN on reactive oxygen species (ROS) and cell survival in cardiomyocytes from WT and MyAkt mice. Murine cardiomyocytes were incubated with TN (3 μg/ml) for 5–6 h *in vitro* before examination. A cohort of WT cardiomyocytes were coincubated with the ER stress inhibitor TUDCA (500 μM), the antioxidant catalase-polyethylene glycol (PEG, 15,000 IU/ml), or the mitochondrial permeation pore (mPTP) inhibitor cyclosporin A (200 nM) at the same time of TN exposure. **(A)**. Representative DCF fluorescent images depicting cardiomyocytes from WT and MyAkt mice treated with TN or TN-treated WT cells in the presence of the ER stress inhibitor TUDCA (500 μM). A cohort of WT cardiomyocytes were coincubated with H_2O_2 (100 μM, positive control) for 5 h in the absence or presence of the antioxidant catalase-PEG; **(B)** ROS production; and **(C)** MTT cell survival. Mean ± SEM, $n = 5$–8 isolations per group, $^{*}p < 0.05$ *versus* WT group; $^{\#}p < 0.05$ *versus* WT-TN group. (To see this illustration in color the reader is referred to the web version of this article at www.liebertonline.com/ars).

apoptosis, mitochondrial damage including loss of mitochondrial membrane potential, and mPTP opening. Intriguingly, intrinsic activation of the essential cell survival molecule Akt mitigated or attenuated the ER stress-induced cardiac contractile and intracellular Ca^{2+} anomalies, ROS accumulation, protein damage, and apoptosis in conjunction with the preserved mitochondrial integrity manifested as restored aconitase activity, mitochondrial membrane potential, and the lessened mPTP opening. Our findings also revealed comparable decreases (all within the range of 32%–41%) in the activation of Akt and GSK3β after ER stress induction both *in vivo* and *in vitro*, the effect of which may be overridden by intrinsic Akt activation and ER stress inhibition by TUDCA. Given that Akt activation was unable to alleviate tunicamycin-induced ER stress (evidenced by the ER stress protein markers *Gadd*153, GRP78, and peIF2α), the beneficial effect of Akt activation against ER stress-induced cardiac anomalies may be attributed to Akt/GSK3β-mediated mitochondrial integrity (rather than ER stress reduction). The involvement of Akt/GSK3β-mediated mitochondrial integrity change in ER stress-induced cardiac mechanical defects was further substantiated by the finding that the mPTP inhibitor cyclosporin A or the GSK3β inhibitor SB216763 prevented ER stress induction-induced cardiomyocyte mechanical and mitochondrial anomalies. Taken together, these results have prompted for a likely role of compromised Akt/GSK3β signaling and subsequent mitochondrial damage in ER stress-induced cardiac contractile dysfunction and the therapeutic potential of Akt in cardiac anomalies under ER stress. A scheme is provided to better illustrate the proposed mechanisms involved in ER stress- and Akt activation-elicited cardiac mechanical and intracellular Ca^{2+} responses (Fig. 11).

Loss of myocardial contractile capacity manifested as compromised cardiac contractility and prolonged diastolic duration are commonly seen in cardiac pathological conditions afflicted with ER stress (11, 17, 25, 31, 32, 35). Our study revealed, for the first time, that induction of ER stress may result in diminished cardiomyocyte contractile function (reduced PS and maximal velocity of shortening/relengthening as well as prolonged relengthening duration) after tunicamycin treatment. This finding supports the notion of an unfavorable role of ER stress in the heart (25, 26, 32) and this is consistent with our current echocardiographic findings of elevated LVESD and reduced factional shortening, similar to a recent report using a somewhat similar rodent model of ER stress (35). Further, our present study noted elevated resting intracellular Ca^{2+} levels, decreased intracellular Ca^{2+} rise in response to electrical-stimulation, and delayed intracellular Ca^{2+} clearance in ER-stressed murine cardiomyocytes, indicating a role of intracellular Ca^{2+} mishandling in ER stress-triggered cardiac contractile dysfunction. The ER stress-induced changes in cardiac contractile and intracellular Ca^{2+} properties seen in our present study were

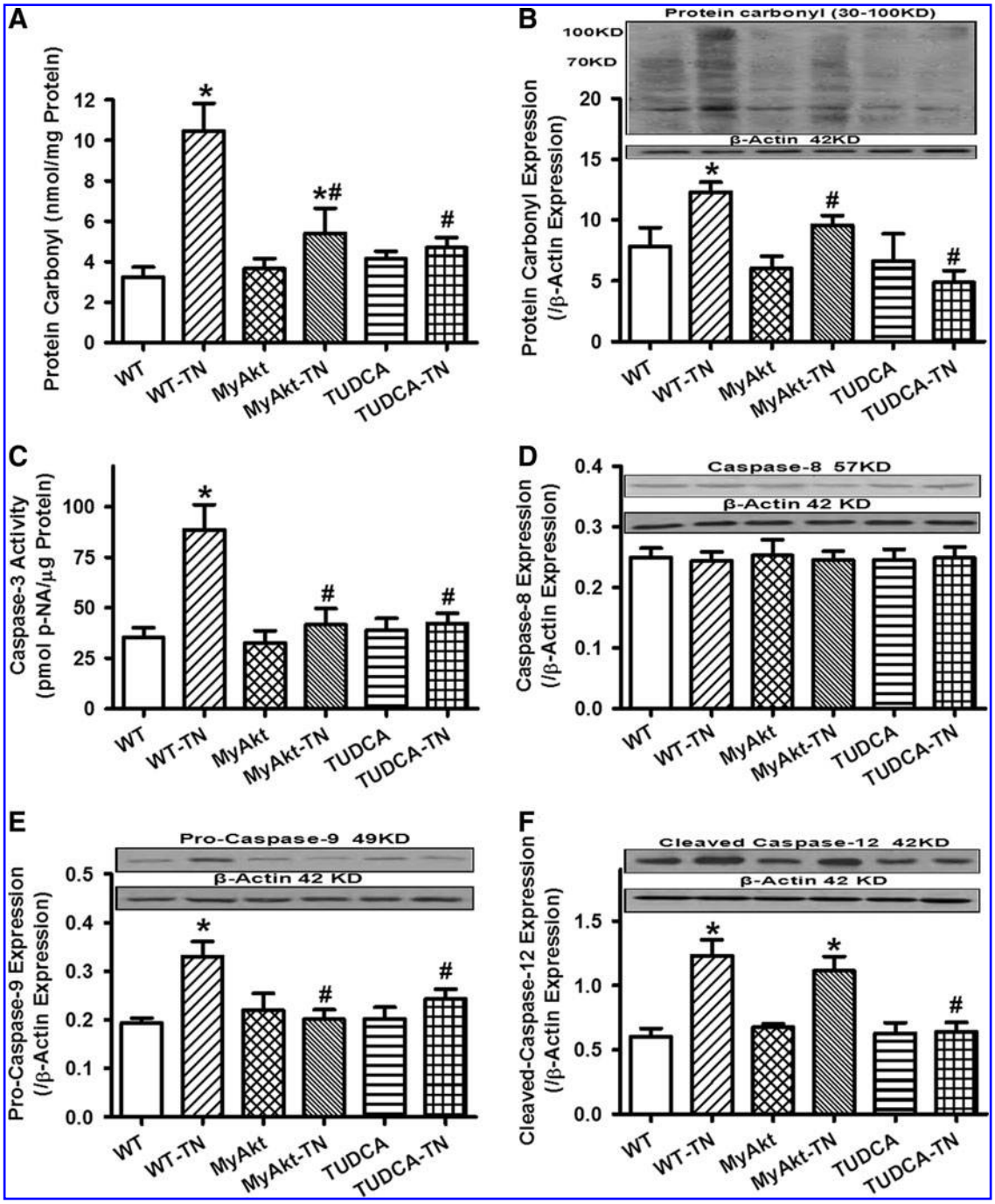

FIG. 8. Effect of TN on protein carbonyl formation and apoptosis (caspase-3 activity, caspase-8, pro-caspase-9, and caspase-12 expression) in cardiomyocytes from adult WT and MyAkt mice. For all *panels* except *panel* **(B)**, murine cardiomyocytes were incubated with TN (3 μg/ml) for 5–6 h *in vitro* before examination. For *panel* **(B)**, TN was injected (3 mg/kg, i.p. for 48 h) *in vivo* along with the ER stress inhibitor TUDCA (50 mg/kg, i.p.). **(A)** Carbonyl formation; **(B)** protein carbonyl expression evaluated by Western blot analysis; **(C)** caspase-3 activity measured by a colorimetric assay; **(D)** caspase-8 expression; **(E)** pro-caspase-9 expression; and **(F)** cleaved caspase-12 expression; *Insets*: Representative gel blots depicting expression of carbonyl, caspase-8, pro-caspase-9, and cleaved caspase-12 using specific antibodies. All protein expression was normalized to that of the loading control β-actin. Mean ± SEM, $n = 5$–8 isolations per group, $^{*}p < 0.05$ *versus* WT group; $^{\#}p < 0.05$ *versus* WT-TN group.

consistent with the previous findings in cardiac pathological conditions where ER stress is abundant (3, 18, 24, 32, 35). These findings have indicated a role of ER stress in compromised cardiac mechanical function under pathological conditions such as cardiac hypertrophy, alcoholism, and sepsis. Our data revealed intracellular Ca^{2+} mishandling after tunicamycin challenge featured by Ca^{2+} overload and compromised intracellular Ca^{2+} extrusion. This is supported by the previous finding that tunicamycin triggers a dramatic increase in intracellular Ca^{2+} concentration, *en route* to alteration in mitochondrial function,

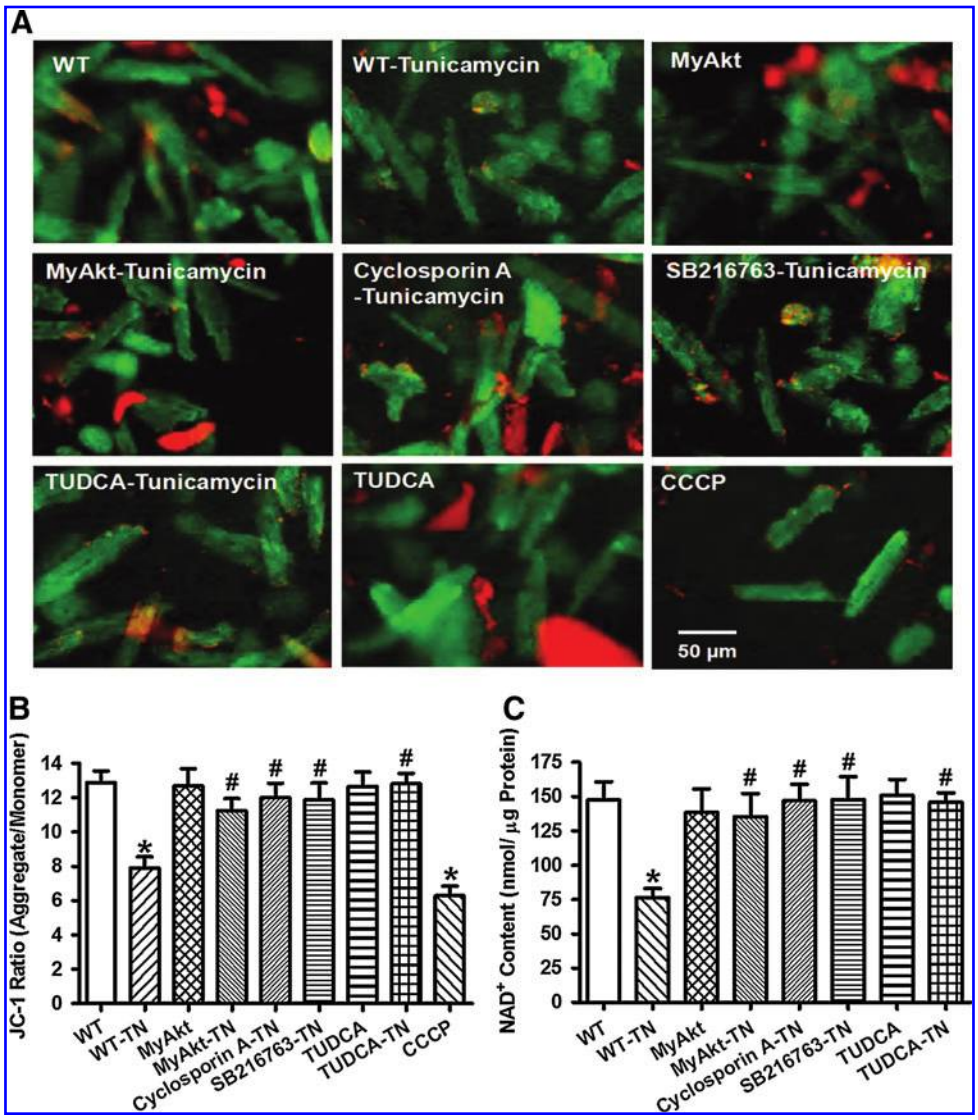

FIG. 9. Effect of TN on mitochondrial integrity using mitochondrial membrane potential and mitochondrial permeability transition pore opening (mPTP) in cardiomyocytes from adult WT and MyAkt mice. Murine cardiomyocytes were incubated with TN (3 μg/ml) for 5–6 h *in vitro* before assessment of mitochondrial function. A cohort of WT cardiomyocytes were coincubated with the mPTP inhibitor cyclosporin A (200 n*M*), the GSK3β inhibitor SB216763 (10 μ*M*), or the ER stress inhibitor TUDCA (500 μ*M*) along with TN exposure. **(A)** Representative JC-1 fluorochrome images depicting mitochondrial membrane potential in the above-mentioned cardiomyocyte groups. The mitochondrial uncoupler carbonyl cyanide m-chlorophenylhydrazone (CCCP) (10 μ*M*) was used as a positive control; **(B)** pooled data of mitochondrial membrane potential (ratio of the red fluorescence obtained at 590 nm to the green fluorescence at 530 nm); and **(C)** mPTP opening evaluated by NAD^+, a marker for mitochondrial permeability transition pore opening; Mean ± SEM, $n = 6$ isolations per group, $^*p < 0.05$ *versus* WT group; $^\#p < 0.05$ *versus* WT-TN group. (To see this illustration in color the reader is referred to the web version of this article at www.liebertonline.com/ars).

and further disturbs intracellular Ca^{2+} homeostasis leading to cell death (6). It is noteworthy that blockade of intracellular Ca^{2+} release abrogates tunicamycin-induced cell injury (6).

Our data depicted overt accumulation of ROS, protein carbonyl formation, apoptosis, and reduced cell survival after tunicamycin challenge, suggesting a possible role of oxidative and protein damage in ER stress-induced cardiac contractile and intracellular Ca^{2+} abnormalities, consistent with the previous notion for a pivotal role of ROS in ER stress-induced cellular damage (23). ROS production and oxidative stress are believed not only coincidental to ER stress, but also essential integral ER stress components that may be turned on by ER stressors to mediate the proapoptotic and proadaptive UPR signaling (3, 11, 40, 47). ROS generation is reported to occur both up- and downstream of UPR targets (3, 40, 47). This is in line with the protective effect of antioxidants against ER stress-induced cellular injury including cardiomyocyte contractility (3, 6, 11, 40). Although it is beyond the scope of our current study, a number of enzymatic mechanisms have been speculated to promote ROS generation under UPR. In particular, the ER oxidoreductases such as flavooxidase Ero1 and protein disulfide isomerase, mitochondrial electron transport, as well as NADPH oxidase including Nox4 have been indicated to mediate ROS generation under ER stress (40). Preliminary findings from our group revealed a significantly upregulated level of NADPH oxidase $p47^{phox}$ subunit after *in vivo* thapsigargin challenge (1 mg/kg, i.p., 48 h), consistent with the beneficial effect of NADPH oxidase inhibition against thapsigargin-induced mitochondrial damage (Zhang Y and Ren J, unpublished data).

Our data revealed that ER stress triggers loss of aconitase activity, mitochondrial membrane potential and mPTP opening associated with reduced Akt-GSK3β phosphorylation. Interestingly, the tunicamycin-induced cardiac dysfunction, mitochondrial damage, and cell death were abolished by inhibition of mPTP opening, favoring a pivotal role of mitochondrial damage in ER stress-induced cardiac anomalies. ER stress has been shown to induce Ca^{2+}-dependent permeability transition, mitochondrial outer membrane permeabilization, and apoptosis in cancer cells (5). Results from our current study revealed that the *N*-linked glycosylation inhibitor tunicamycin is capable of interrupting cardiac

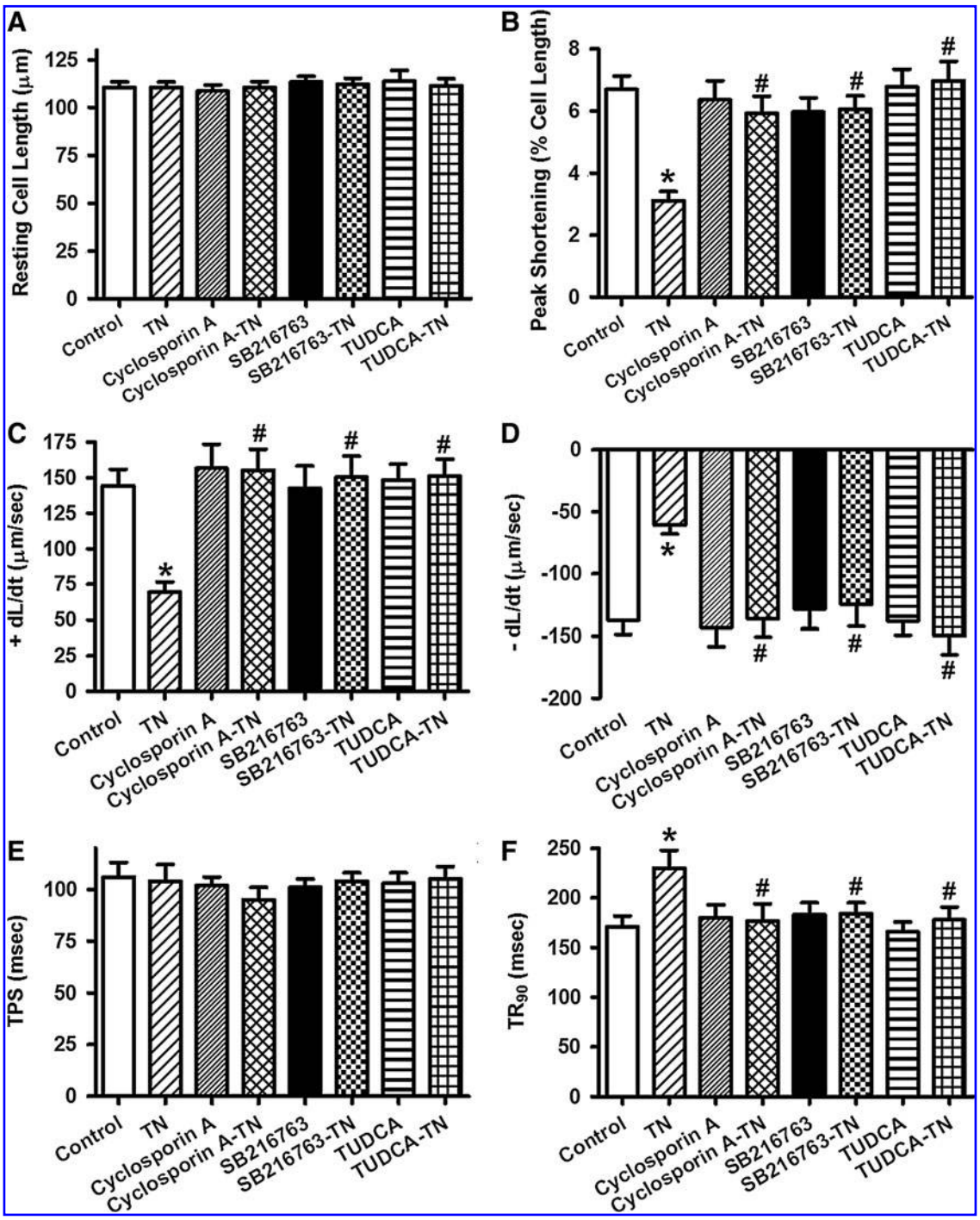

FIG. 10. Effect of the mPTP inhibitor cyclosporine A, the GSK3β inhibitor SB216763 and the ER stress inhibitor TUDCA on TN-induced cardiomyocyte contractile dysfunction. Freshly isolated murine cardiomyocytes were incubated with TN (3 μg/ml) for 5–6 h *in vitro* in the absence or presence of cyclosporine A (200 n*M*), SB216763 (10 μ*M*), or TUDCA (500 μ*M*) before assessment of mechanical properties. **(A)** Resting cell length; **(B)** PS (% of resting cell length); **(C)** maximal velocity of shortening (+dL/dt); **(D)** maximal velocity of relengthening (−dL/dt); **(E)** TPS; and **(F)** time-to-90% relengthening (TR_{90}). Mean ± SEM, $n = 52$–53 cells per group, $^{*}p < 0.05$ *versus* control (without drug treatment) group; $^{\#}p < 0.05$ *versus* TN group.

contractile function through mitochondrial damage-mediated apoptosis. ROS generation has been shown to occur both up- and downstream of mitochondria. Antioxidants may inhibit ROS production and protect against tunicamycin-induced mitochondrial depolarization in Leishmania cells (6). On the other hand, mitochondrial damage is known to further trigger ROS generation (40). Our data revealed reduced Akt phosphorylation under ER stress. Although the precise mechanism is still unclear for the dampened Akt activation under ER stress in the heart, ER stress has been shown to promote apoptosis through suppression of phosphatidylinositol 3-kinase (PI-3 kinase), an upstream signaling molecule of Akt, in

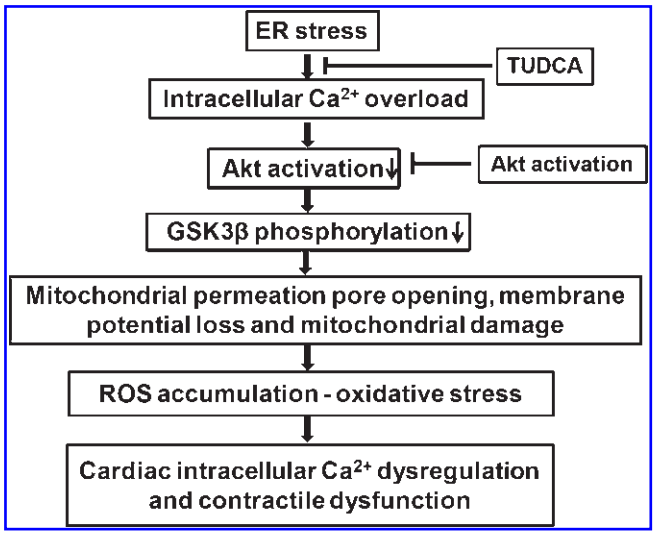

FIG. 11. Schematic diagram depicting ER stress-induced cellular events leading to mitochondrial damage, intracellular Ca^{2+} dysregulation, and contractile dysfunction in the heart as well as how chronic Akt activation may rescue the heart from ER stress-induced cardiac anomalies. TUDCA (an ER chaperon to inhibit ER stress). Please note that intracellular Ca^{2+} overload and dysregulation may occur immediately after induction of ER stress and/or as the final instigator to trigger cardiac contractile dysfunction after onset of mitochondrial damage and ROS production. Also note that ROS production and mitochondrial damage may happen in a reciprocal manner, leading to a vicious cycle for ROS accumulation.

mouse insulinoma cells (42). GSK3β, a serine/threonine kinase downstream of Akt, is known to govern mPTP opening in pathological conditions such as aging, diabetes, and ischemia-reperfusion (24, 46, 48). Phosphorylation of Akt and GSK3β has been shown to prevent mPTP opening and thus inhibit cell death (8, 46, 48). Our data depicted lessened GSK3β phosphorylation, denoting a higher GSK3β kinase activity and increased propensity of mPTP opening in ER stress, which is supported by the finding that pharmacological inhibition of either GSK3β or mPTP opening reconciled tunicamycin-induced cardiomyocyte contractile and mitochondrial dysfunction, in a manner reminiscent to the ER stress chaperon TUDCA. Last but not the least, the involvement of ER stress-associated mitochondrial damage is further supported by the upregulated mitochondrial death protein pro-caspase-9 and ER stress-specific apoptotic protein caspase-12 (28) but not the death receptor protein caspase-8. In particular, tunicamycin induced upregulation of caspase-12, favoring a role of the ER stress-specific caspase-12 in ER stress-induced apoptosis, protein, and cell damage.

Perhaps the most intriguing finding from our study is that intrinsic Akt activation mitigated the ER stress-induced cardiac contractile defect, intracellular Ca^{2+} mishandling, ROS production, protein damage, apoptosis, and mitochondrial damage, in a manner reminiscent of the ER chaperon TUDCA. Moreover, intrinsic Akt activation also improved phosphorylation of Akt and GSK3β under ER stress. These data favor a prominent role of Akt activation and subsequently inactivation of GSK3β (via GSK3β phosphorylation) in the preserved cardiomyocyte function, cell survival, and mitochondrial integrity under ER stress. Several mechanisms may be speculated for Akt activation-elicited protection against ER stress-induced cardiac mechanical, mitochondrial, and intracellular Ca^{2+} anomalies. First, our data revealed that Akt may exert its beneficial effect simply through normalizing intracellular Ca^{2+} homeostasis, as intracellular Ca^{2+} overloading and dysregulation are responsible for ER stress-induced perturbation of cell function. Second, our findings depicted that Akt activation ameliorated ER stress-induced ROS production, protein damage, and apoptosis, suggesting a possible regulatory mechanism of ROS, protein damage, and apoptosis in Akt-offered beneficial responses against ER stress. Third, intrinsic Akt activation is capable of lessening ER stress-induced cardiac abnormality by preventing GSK3β-mediated mitochondrial damage (loss of aconitase activity, mitochondrial membrane potential, and mPTP opening), favoring a key role of mitochondria in Akt activation-offered cardioprotection. Enhanced mitochondrial damage, oxidative stress, and apoptosis have been shown to promote protein damage and interrupt cardiac contractile function (4, 10). Akt activation ablated tunicamycin-induced elevation in pro-caspase-9 but not the ER-specific caspase-12, and this depicts a mitochondria-dependent, rather than caspase-12-dependent, apoptotic mechanism for Akt. Two machineries operate independent of one another in ER stress-induced apoptosis with one being mitochondria-dependent apoptotic pathway and the other being the caspase-12-dependent apoptotic pathway (6, 28). In addition, our observation that GSK3β inhibitor SB216763 and mPTP inhibitor cyclosprin A mimicked Akt activation-induced protection against ER stress further consolidates the role of GSK3β-governed mPTP opening and mitochondrial integrity in the maintenance of cardiomyocyte physiology. GSK3β is known to interact with components of the mPTP, voltage-dependent anion channel (VDAC), and adenine nucleotide translocase to modulate mPTP opening and mitochondrial membrane depolarization (13). Our data revealed that Akt activation itself did not significantly affect cardiomyocyte mechanical and intracellular Ca^{2+} properties as well as the biochemical indices tested in our study, indicating that activation of this essential survival factor early on in life may not be innately harmful to myocardial function. A previous report using much younger MyAkt mice (10–15 weeks old) indicated a decreased capacity of cardiac function recovery after myocardial infarction (27). Nonetheless, systolic ventricular function is preserved in these MyAkt mice at the same age (9–19 weeks old) accompanied with protection to massive cardiac dilatation and sudden death (22). The subtle difference in cardiac function between the earlier (27) and current study may be related to factors, including function assessment technique (Langendorff heart in (27) *vs.* echocardiographic and cardiomyocytes used in our study) and the apparent difference in mouse age [10–15 weeks of age used in (27)]. Last but not the least, Akt activation failed to alter the ER stress status triggered by tunicamycin, indicating that the beneficial effect of Akt does not occur through direct neutralizing effect against ER stress as the chemical chaperon TUDCA.

Experimental limitations: One of the major limitations of this study is that almost all data relied on pharmacological approach to modulate ER stress. Given that genetic models of ER stress have been generated (12, 21), further study should be carried out using murine genetic models of ER stress to assess the role of Akt and GSK3β in the regulation of cardiac

contractile and mitochondrial function. Further, although our data favor an essential role of ROS and intracellular Ca^{2+} mishandling in ER stress-induced cardiac dysfunction, the interaction and signaling process (*e.g.*, to regulate the Akt/GSK3β signaling) between the ER and mitochondria still remain elusive. It was reported that the mitochondrial protein regulating mPTP opening VDAC is physically linked to the ER Ca^{2+}-release channel inositol 1,4,5-trisphosphate receptor through the molecular chaperone glucose-regulated protein 75 (43), highlighting chaperone-mediated conformational coupling between ER Ca^{2+} release channel and mitochondria. Further study is warranted to examine the impact of Akt or its downstream signals on this ER–mitochondria interaction and subsequently localized Ca^{2+} levels and mitochondrial integrity.

ER stress has been considered as a main player contributing to a wide variety of cardiac pathologies (9, 14). Our current finding suggests that Akt plays an essential role in the preservation of cardiac contractile function against ER stress possibly through alleviating GSK3β-mediated mitochondrial damage. Further, our data depict an ER stress-associated decline in the phosphorylation of Akt-GSK3β signaling cascade, suggesting a potential therapeutic target for Akt-GSK3β signaling in ER stress-associated cardiac anomalies. Although our study sheds some light on the interaction of oxidative stress, mitochondrial integrity, and ER stress-associated mechanical and intracellular Ca^{2+} defects, the precise mechanisms of action behind ER stress-mediated cardiac pathologies still deserve further in-depth investigation.

Materials and Methods

Mice with cardiac-specific overexpression of Akt and in vivo *ER stress*

All experimental procedures were approved by the Animal Care and Use Committee at the University of Wyoming (Laramie, WY). Mice overexpressing the hemagglutinin-tagged Akt (MyAkt) with src myristoylation signal under the direction of the murine α-myosin heavy chain promoter were kindly provided by Dr. Anthony Rosenzweig (Harvard Medical School, Boston, MA). The cDNA encoding MyAkt was subcloned downstream of the 5.5-kb murine α-myosin heavy chain promoter and was used to generate cardiac-specific transgenic mice through oocyte injection. Positive founders were identified by Southern blotting and bred to wild-type (WT) mice. MyAkt transgenic mice were genotyped by PCR (data shown in Supplementary Fig. S2) (22). Adult (8–10 months old) male MyAkt and WT mice (26 ± 2 g) were used for the study. The rationale for using 8–10 months of age was essentially a more stable Akt activation level after the first 6 months of life in these mice based on our age-related screening. To elicit ER stress *in vivo*, mice were injected with tunicamycin, an inhibitor of *N*-glycosylation in the ER (1 or 3 mg/kg, i.p.) for 48 h before assessment of mechanical properties (30, 35, 44, 45). Control mice received similar amount of saline (i.p.). All mice were maintained with a 12/12-light/dark cycle with free access to tap water and rodent chow until experimentation.

Isolation of murine cardiomyocytes and induction of ER stress in vitro

Hearts were rapidly removed from anesthetized (ketamine 80 mg/kg and xylazine 12 mg/kg, i.p.) mice and mounted onto a temperature-controlled (37°C) Langendorff system. After perfusion with a modified Tyrode's solution (Ca^{2+} free) for 2 min, the heart was digested with a Ca^{2+}-free KHB buffer containing liberase blendzyme 4 (Hoffmann-La Roche, Inc., Indianapolis, IN) for 20 min. The modified Tyrode's solution (pH 7.4) contained the following (in mM): NaCl 135, KCl 4.0, $MgCl_2$ 1.0, HEPES 10, NaH_2PO4 0.33, glucose 10, and butanedione monoxime 10. The solution was gassed with 5% CO_2–95% O_2. The digested heart was removed from the cannula and left ventricle was cut into small pieces in the modified Tyrode's solution. Tissue pieces were gently agitated and pellet of cells was resuspended. Extracellular Ca^{2+} was added incrementally back to 1.20 m*M* over 30 min. A yield of at least 50%–60% viable rod-shaped cells with clear sacromere striations was achieved. Cardiomyocytes with obvious sarcolemmal blebs or spontaneous contraction were not chosen for mechanical examination (7). To induce ER stress *in vitro*, murine cardiomyocytes were incubated with tunicamycin (3 μg/ml) or saline (for controls) for 5–6 h at 37°C before assessment of mechanical, biochemical, and protein properties at room temperature unless otherwise stated (30, 44). To directly assess the effect of mPTP and GSK3β on ER stress-induced cardiac dysfunction, cardiomyocytes were incubated at 37°C with tunicamycin (3 μg/ml) in the absence or presence of the mPTP inhibitor cyclosporine A (200 n*M*) (41), the GSK3β inhibitor SB216763 (10 μ*M*) (13), or the ER stress chaperon TUDCA (500 μ*M*, as a positive control) (11) before mechanical assessment at room temperature.

Echocardiographic assessment

Cardiac geometry and function were evaluated in anesthetized (Avertin 2.5%, 10 μl/g body weight, i.p.) mice using 2-D guided M-mode echocardiography (Sonos 5500) equipped with a 15-6 MHz linear transducer. Avertin is approved as a survival anesthetic that provides rapid induction and recovery for single use or short duration (approximately 15–20 min) surgical procedures in mice (34). LV anterior and posterior wall dimensions during diastole and systole were recorded from three consecutive cycles in M-mode using methods adopted by the American Society of Echocardiography. Fractional shortening was calculated from LVEDD and LVESD diameters using the equation (LVEDD – LVESD)/LVEDD (38).

Cell shortening/relengthening

Mechanical properties of cardiomyocytes were assessed using a SoftEdge MyoCam® system (IonOptix Corporation, Milton, MA). In brief, cells were placed in a Warner chamber mounted on the stage of an inverted microscope (Olympus, IX-70) and superfused ($\sim$1 ml/min at 25°C) with a buffer containing (in mM): 131 NaCl, 4 KCl, 1 $CaCl_2$, 1 $MgCl_2$, 10 glucose, and 10 HEPES, at pH 7.4. Room temperature was chosen for mechanical study due to a longer working window as a result of slower metabolism. The cells were field stimulated with supra-threshold voltage at a frequency of 0.5 Hz (unless otherwise stated), 3 ms duration, using a pair of platinum wires placed on opposite sides of the chamber connected to an FHC stimulator (Brunswick, NE). The myocyte being studied was displayed on the computer monitor using an IonOptix MyoCam camera. IonOptix SoftEdge software was used to capture changes in cell length during shortening

and relengthening. Cell shortening and relengthening were assessed using the following indices: PS—indicative of ventricular contractility; time-to-PS (TPS)—indicative of contraction duration; time-to-90% relengthening (TR_{90})—representing relaxation duration; maximal velocities of shortening (+dL/dt) and relengthening (−dL/dt)—indicatives of maximal velocities of ventricular pressure rise/fall (2).

Intracellular Ca^{2+} transient measurement

Myocytes were loaded with fura-2/AM (0.5 μM) for 10 min and fluorescence measurements were recorded with a dual-excitation fluorescence photomultiplier system (IonOptix). Cardiomyocytes were placed on an Olympus IX-70 inverted microscope and imaged through a Fluor ×40 oil objective. Cells were exposed to light emitted by a 75W lamp and passed through either a 360 or a 380 nm filter, while being stimulated to contract at 0.5 Hz. Fluorescence emissions were detected between 480 and 520 nm by a photomultiplier tube after first illuminating the cells at 360 nm for 0.5 s then at 380 nm for the duration of the recording protocol (333 Hz sampling rate). The 360 nm excitation scan was repeated at the end of the protocol and qualitative changes in intracellular Ca^{2+} concentration were inferred from the ratio of fura-2 fluorescence intensity at two wavelengths (360/380). Fluorescence decay time was measured as an indication of the intracellular Ca^{2+} clearing rate. Both single and biexponential curve fit programs were applied to calculate the intracellular Ca^{2+} decay constant (7).

Aconitase activity

Mitochondrial aconitase, an iron-sulfur enzyme located in citric acid cycle, is readily damaged by oxidative stress *via* removal of an iron from [4Fe-4S] cluster. Mitochondrial fractions prepared from whole heart homogenate were resuspended in 0.2 m*M* sodium citrate. Aconitase activity assay (Aconitase activity assay kit, Aconitase-340 assay™; OxisResearch, Portland, OR) was performed according to manufacturer's instructions with minor modifications. Briefly, mitochondrial sample (50 μl) was mixed in a 96-well plate with 50 μl trisodium citrate (substrate) in Tri-HCl pH 7.4, 50 μl isocitrate dehydrogenase (enzyme) in Tris-HCl, and 50 μl NADP in Tris-HCl. After incubating for 15 min at 37°C, the absorbance was dynamically recorded at 340 nm every min for 5 min with a spectrophotometer. During the assay, citrate is isomerized by aconitase into isocitrate and eventually α-ketoglutarate. The Aconitase-340 assay™ measures NADPH formation, a product of the oxidation of isocitrate to α-ketoglutarate. Tris-HCl buffer (pH 7.4) was served as blank (37).

Intracellular ROS

Production of ROS was evaluated by fluorescence intensity changes resulting from oxidation of the intracellular fluoroprobe 5-(6)-chloromethyl-2′,7′-dichlorodihydrofluorescein diacetate (CM-H_2DCFDA). In brief, isolated cardiomyocytes from WT and MyAkt mice were incubated with tunicamycin (3 μg/ml) at 37°C for 5–6 h. A cohort of WT cardiomyocytes were coincubated with the ER stress inhibitor TUDCA (500 μM), or the antioxidant catalase-PEG (15,000 IU/ml) (36) at the same time with tunicamycin. H_2O_2 (100 μM) was used as the positive control in the absence or presence of the antioxidant catalase-PEG. Cardiomyocytes were then loaded with the nonfluorescent dye 2′,7′-dichlorodihydrofluorescein diacetate (H_2DCFDA, 1 μM; Molecular Probes, Eugene, OR) at 37°C for 30 min. The myocytes were rinsed and the fluorescence intensity was then measured using a fluorescent microplate reader at an excitation wavelength of 480 nm and an emission wavelength of 530 nm. Untreated cardiomyocytes without fluorescence were used to determine the background fluorescence. The final fluorescent intensity was normalized to protein content in each cardiomyocyte group measured using the Bradford assay (1).

MTT assay for cell viability

[3-(4,5-Dimethylthiazol-2-yl)-2,5-diphenyltetrazolium bromide] (MTT) assay is based on transformation of the tetrazolium salt MTT by active mitochondria to an insoluble formazan salt. Although MTT assay may not be as sensitive as LDH release in cytoplasm to evaluate cell viability, the fact that MTT is reduced to purple formazan by succinate dehydrogenase in mitochondria makes it a better choice for assessment of mitochondrial function (19). Cardiomyocytes (with or without induction of ER stress) were plated in microtiter plate at a density of 3×10^5 cells/ml. MTT was added to each well with a final concentration of 0.5 mg/ml, and the plates were incubated for 2 h at 37°C. The formazan crystals in each well were dissolved in dimethyl sulfoxide (150 μl/well). Formazan was quantified spectroscopically at 560 nm using a SpectraMax® 190 spectrophotometer (16).

Protein carbonyl assay

Proteins were extracted from cardiomyocytes and nucleic acids were eliminated by treating the samples with 1% streptomycin sulfate for 15 min, followed by a 10 min centrifugation (11,000 *g*). Protein was precipitated by adding an equal volume of 20% trichloroacetic acid (TCA) to protein (0.5 mg) and centrifuged for 1 min. The TCA solution was removed and the sample resuspended in 10 m*M* 2,4-dinitrophenylhydrazine (2,4-DNPH) solution. Samples were incubated at room temperature for 15–30 min. After adding 500 μl of 20% TCA, samples were centrifuged for 3 min. The supernatant was discarded, the pellet washed in ethanol: ethyl acetate and allowed to incubate at room temperature for 10 min. The samples were centrifuged again for 3 min and the ethanol: ethyl acetate steps repeated twice. The precipitate was resuspended in 6 *M* guanidine solution and centrifuged for 3 min, and any insoluble debris removed. The maximum absorbance (360–390 nm) of supernatant was read against appropriate blanks (water, 2 *M* HCl) and the carbonyl content was calculated using the molar absorption coefficient of 22,000 M^{-1} cm^{-1} (38).

Caspase-3 assay

Caspase-3 is an enzyme activated during induction of apoptosis. In brief, 1 ml of PBS was added to flasks containing mouse cardiomyocytes and the monolayer was scraped and collected in a microfuge tube. The cells were centrifuged at 10,000 *g* at 4°C for 10 min and cell pellets were lysed in 100 μl of ice-cold cell lysis buffer (50 m*M* HEPES, 0.1% CHAPS, 1 m*M* dithiothreitol, 0.1 m*M* EDTA, and 0.1% NP40). After cells were lysed, 70 μl of reaction buffer was added to cell lysate (30 μl) followed by an additional 20 μl of caspase-3

colorimetric substrate (Ac-DEVD-pNA) and incubated at 37°C for 1 h, during which time the caspase in the sample was allowed to cleave the chromophore p-NA from the substrate molecule. The samples were then read with a microplate reader at 405 nm. Caspase-3 activity was expressed as picomoles of pNA released per microgram of protein per minute (7).

Measurement of mitochondrial membrane potential

Murine cardiomyocytes were suspended in HEPES-saline buffer and mitochondrial membrane potential ($\Delta\Psi_m$) was detected as described (20). Briefly, after incubation with JC-1 (5 μM) for 10 min at 37°C, cells were rinsed twice by sedimentation using the HEPES saline buffer free of JC-1 before being examined under a confocal laser scanning microscope (Leica TCS SP2) at excitation wavelength of 490 nm. The emission of fluorescence was recorded at 530 nm (monomer form of JC-1, green) and at 590 nm (aggregate form of JC-1, red). Results in fluorescence intensity were expressed as 590-to-530-nm emission ratio. The mitochondrial uncoupler carbonyl cyanide m-chlorophenylhydrazone (10 μM) was used as a positive control for mitochondrial membrane potential measurement.

Determination of mPTP opening

mPTP opening was determined using NAD^+, a marker of mPTP opening. In brief, pellets of cardiomyocytes were mixed thoroughly in liquid nitrogen with perchloric acid (0.6 *M*). The mixture was homogenized, neutralized with potassium hydroxide (3 *M*), and centrifuged. NAD^+ concentrations were determined fluorometrically in dilutions of the supernatant sample using alcohol dehydrogenase with an excitation wavelength of 339 nm and emission wavelength of 460 nm (48).

Western blot analysis

Pellets of cardiomyocytes were sonicated in a lysis buffer containing 20 m*M* Tris (pH 7.4), 150 m*M* NaCl, 1 m*M* EDTA, 1 m*M* EGTA, 1% Triton, 0.1% sodium dodecyl sulfate (SDS), and a protease inhibitor cocktail. Protein levels of the ER stress markers *Gadd*153, GRP78, and phosphorylated eIF2α (peIF2α), apoptotic markers caspase-8 and pro-caspase-9, Akt, pAkt, GSK3β, and phosphorylated GSK3β (pGSK3β) were examined by standard Western immunoblotting. Membranes were probed with anti-*Gadd*153 (1:500), anti-GRP78 (1:1000), anti-peIF2α (Ser^{51}, 1:1000), anti-caspase-8 (1:1000), anti-pro-caspase-9 (1:1000), anti-cleaved caspase-12 (1:1000), anti-dinitrophenyl (1:150; for detection of protein carbonyl); anti-Akt (1:1000), anti-pAkt (Thr^{473}, 1:1000), anti-GSK3β (1:1000), anti-pGSK3β (Ser^{9}, 1:1000), and anti-β-actin (loading control, 1:2000) antibodies. Antibodies were purchased from Cell Signaling Technology (Beverly, MA), Santa Cruz Biotechnology (Santa Cruz, CA), or Millipore (Billerica, MA). The membranes were incubated with horseradish peroxidase-coupled secondary antibodies. After immunoblotting, the film was scanned and detected with a Bio-Rad Calibrated Densitometer (38).

Data analysis

Data were mean ± SEM. Statistical significance ($p < 0.05$) was estimated by one-way analysis of variance followed by a Tukey's test for *post hoc* analysis.

Acknowledgments

The authors wish to gratefully acknowledge Drs. Feng Dong, Ming Yuan, and Qun Li from University of Wyoming (Laramie, WY) for their skillful technical assistance. Part of this work was presented at the American Heart Association Scientific Session in Orlando, FL (2007). This work was supported in part by NIH/NCRR P20 RR016474 (J.R.).

Author Disclosure Statement

None of the authors declare any conflict of interest associated with this work.

References

1. Bradford MM. A rapid and sensitive method for the quantitation of microgram quantities of protein utilizing the principle of protein-dye binding. *Anal Biochem* 72: 248–254, 1976.
2. Ceylan-Isik AF, Sreejayan N, and Ren J. Endoplasmic reticulum chaperon tauroursodeoxycholic acid alleviates obesity-induced myocardial contractile dysfunction. *J Mol Cell Cardiol* 50: 107–116, 2011.
3. Ceylan-Isik AF, Zhao P, Zhang B, Xiao X, Su G, and Ren J. Cardiac overexpression of metallothionein rescues cardiac contractile dysfunction and endoplasmic reticulum stress but not autophagy in sepsis. *J Mol Cell Cardiol* 48: 367–378, 2010.
4. Chien KR. Stress pathways and heart failure. *Cell* 98: 555–558, 1999.
5. Deniaud A, Sharaf El DO, Maillier E, Poncet D, Kroemer G, Lemaire C, and Brenner C. Endoplasmic reticulum stress induces calcium-dependent permeability transition, mitochondrial outer membrane permeabilization and apoptosis. *Oncogene* 27: 285–299, 2008.
6. Dolai S, Pal S, Yadav RK, and Adak S. Endoplasmic reticulum stress-induced apoptosis in Leishmania through CA2+-dependent and caspase-independent mechanism. *J Biol Chem* 286: 13638–13646, 2011.
7. Doser TA, Turdi S, Thomas DP, Epstein PN, Li SY, and Ren J. Transgenic overexpression of aldehyde dehydrogenase-2 rescues chronic alcohol intake-induced myocardial hypertrophy and contractile dysfunction. *Circulation* 119: 1941–1949, 2009.
8. Feng J, Lucchinetti E, Ahuja P, Pasch T, Perriard JC, and Zaugg M. Isoflurane postconditioning prevents opening of the mitochondrial permeability transition pore through inhibition of glycogen synthase kinase 3beta. *Anesthesiology* 103: 987–995, 2005.
9. Glembotski CC. Endoplasmic reticulum stress in the heart. *Circ Res* 101: 975–984, 2007.
10. Goldhaber JI and Qayyum MS. Oxygen free radicals and excitation-contraction coupling. *Antioxid Redox Signal* 2: 55–64, 2000.
11. Guo R, Ma H, Gao F, Zhong L, and Ren J. Metallothionein alleviates oxidative stress-induced endoplasmic reticulum stress and myocardial dysfunction. *J Mol Cell Cardiol* 47: 228–237, 2009.
12. Iwawaki T, Akai R, Kohno K, and Miura M. A transgenic mouse model for monitoring endoplasmic reticulum stress. *Nat Med* 10: 98–102, 2004.
13. Javadov S, Rajapurohitam V, Kilic A, Zeidan A, Choi A, and Karmazyn M. Anti-hypertrophic effect of NHE-1 inhibition involves GSK-3beta-dependent attenuation of

mitochondrial dysfunction. *J Mol Cell Cardiol* 46: 998–1007, 2009.
14. Kitakaze M and Tsukamoto O. What is the role of ER stress in the heart? Introduction and series overview. *Circ Res* 107: 15–18, 2010.
15. Lee Y and Gustafsson AB. Role of apoptosis in cardiovascular disease. *Apoptosis* 14: 536–548, 2009.
16. Li Q, Yang X, Sreejayan N, and Ren J. Insulin-like growth factor I deficiency prolongs survival and antagonizes paraquat-induced cardiomyocyte dysfunction: role of oxidative stress. *Rejuvenation Res* 10: 501–512, 2007.
17. Li SY, Gilbert SA, Li Q, and Ren J. Aldehyde dehydrogenase-2 (ALDH2) ameliorates chronic alcohol ingestion-induced myocardial insulin resistance and endoplasmic reticulum stress. *J Mol Cell Cardiol* 47: 247–255, 2009.
18. Li SY and Ren J. Cardiac overexpression of alcohol dehydrogenase exacerbates chronic ethanol ingestion-induced myocardial dysfunction and hypertrophy: role of insulin signaling and ER stress. *J Mol Cell Cardiol* 44: 992–1001, 2008.
19. Lobner D. Comparison of the LDH and MTT assays for quantifying cell death: validity for neuronal apoptosis? *J Neurosci Methods* 96: 147–152, 2000.
20. Ma H, Li SY, Xu P, Babcock SA, Dolence EK, Brownlee M, Li J, and Ren J. Advanced glycation endproduct (AGE) accumulation and AGE receptor (RAGE) up-regulation contribute to the onset of diabetic cardiomyopathy. *J Cell Mol Med* 13: 1751–1764, 2009.
21. Mao C, Dong D, Little E, Luo S, and Lee AS. Transgenic mouse model for monitoring endoplasmic reticulum stress *in vivo*. *Nat Med* 10: 1013–1014, 2004.
22. Matsui T, Li L, Wu JC, Cook SA, Nagoshi T, Picard MH, Liao R, and Rosenzweig A. Phenotypic spectrum caused by transgenic overexpression of activated Akt in the heart. *J Biol Chem* 277: 22896–22901, 2002.
23. Merksamer PI, Trusina A, and Papa FR. Real-time redox measurements during endoplasmic reticulum stress reveal interlinked protein folding functions. *Cell* 135: 933–947, 2008.
24. Miki T, Miura T, Hotta H, Tanno M, Yano T, Sato T, Terashima Y, Takada A, Ishikawa S, and Shimamoto K. Endoplasmic reticulum stress in diabetic hearts abolishes erythropoietin-induced myocardial protection by impairment of phospho-glycogen synthase kinase-3beta-mediated suppression of mitochondrial permeability transition. *Diabetes* 58: 2863–2872, 2009.
25. Minamino T and Kitakaze M. ER stress in cardiovascular disease. *J Mol Cell Cardiol* 48: 1105–1110, 2010.
26. Minamino T, Komuro I, and Kitakaze M. Endoplasmic reticulum stress as a therapeutic target in cardiovascular disease. *Circ Res* 107: 1071–1082, 2010.
27. Nagoshi T, Matsui T, Aoyama T, Leri A, Anversa P, Li L, Ogawa W, del MF, Gwathmey JK, Grazette L, Hemmings BA, Kass DA, Champion HC, and Rosenzweig A. PI3K rescues the detrimental effects of chronic Akt activation in the heart during ischemia/reperfusion injury. *J Clin Invest* 115: 2128–2138, 2005.
28. Nakagawa T, Zhu H, Morishima N, Li E, Xu J, Yankner BA, and Yuan J. Caspase-12 mediates endoplasmic-reticulum-specific apoptosis and cytotoxicity by amyloid-beta. *Nature* 403: 98–103, 2000.
29. Ni M and Lee AS. ER chaperones in mammalian development and human diseases. *FEBS Lett* 581: 3641–3651, 2007.
30. Nickson P, Toth A, and Erhardt P. PUMA is critical for neonatal cardiomyocyte apoptosis induced by endoplasmic reticulum stress. *Cardiovasc Res* 73: 48–56, 2007.
31. Okada K, Minamino T, and Kitakaze M. [Role of endoplasmic reticulum stress in hypertrophic and failing hearts]. *Nippon Yakurigaku Zasshi* 126: 385–389, 2005.
32. Okada K, Minamino T, Tsukamoto Y, Liao Y, Tsukamoto O, Takashima S, Hirata A, Fujita M, Nagamachi Y, Nakatani T, Yutani C, Ozawa K, Ogawa S, Tomoike H, Hori M, and Kitakaze M. Prolonged endoplasmic reticulum stress in hypertrophic and failing heart after aortic constriction: possible contribution of endoplasmic reticulum stress to cardiac myocyte apoptosis. *Circulation* 110: 705–712, 2004.
33. Ozcan U, Yilmaz E, Ozcan L, Furuhashi M, Vaillancourt E, Smith RO, Gorgun CZ, and Hotamisligil GS. Chemical chaperones reduce ER stress and restore glucose homeostasis in a mouse model of type 2 diabetes. *Science* 313: 1137–1140, 2006.
34. Papaioannou VE and Fox JG. Efficacy of tribromoethanol anesthesia in mice. *Lab Anim Sci* 43: 189–192, 1993.
35. Petrovski G, Das S, Juhasz B, Kertesz A, Tosaki A, and Das DK. Cardioprotection by endoplasmic reticulum stress-induced autophagy. *Antioxid Redox Signal* 14: 2191–2200, 2011.
36. Privratsky JR, Wold LE, Sowers JR, Quinn MT, and Ren J. AT1 blockade prevents glucose-induced cardiac dysfunction in ventricular myocytes: role of the AT1 receptor and NADPH oxidase. *Hypertension* 42: 206–212, 2003.
37. Relling DP, Esberg LB, Fang CX, Johnson WT, Murphy EJ, Carlson EC, Saari JT, and Ren J. High-fat diet-induced juvenile obesity leads to cardiomyocyte dysfunction and upregulation of Foxo3a transcription factor independent of lipotoxicity and apoptosis. *J Hypertens* 24: 549–561, 2006.
38. Ren J, Privratsky JR, Yang X, Dong F, and Carlson EC. Metallothionein alleviates glutathione depletion-induced oxidative cardiomyopathy in murine hearts. *Crit Care Med* 36: 2106–2116, 2008.
39. Ron D and Walter P. Signal integration in the endoplasmic reticulum unfolded protein response. *Nat Rev Mol Cell Biol* 8: 519–529, 2007.
40. Santos CX, Tanaka LY, Wosniak J, and Laurindo FR. Mechanisms and implications of reactive oxygen species generation during the unfolded protein response: roles of endoplasmic reticulum oxidoreductases, mitochondrial electron transport, and NADPH oxidase. *Antioxid Redox Signal* 11: 2409–2427, 2009.
41. Saotome M, Katoh H, Yaguchi Y, Tanaka T, Urushida T, Satoh H, and Hayashi H. Transient opening of mitochondrial permeability transition pore by reactive oxygen species protects myocardium from ischemia-reperfusion injury. *Am J Physiol Heart Circ Physiol* 296: H1125–H1132, 2009.
42. Srinivasan S, Ohsugi M, Liu Z, Fatrai S, Bernal-Mizrachi E, and Permutt MA. Endoplasmic reticulum stress-induced apoptosis is partly mediated by reduced insulin signaling through phosphatidylinositol 3-kinase/Akt and increased glycogen synthase kinase-3beta in mouse insulinoma cells. *Diabetes* 54: 968–975, 2005.
43. Szabadkai G, Bianchi K, Varnai P, De SD, Wieckowski MR, Cavagna D, Nagy AI, Balla T, and Rizzuto R. Chaperone-mediated coupling of endoplasmic reticulum and mitochondrial Ca2+ channels. *J Cell Biol* 175: 901–911, 2006.
44. Wei H, Zhang R, Jin H, Liu D, Tang X, Tang C, and Du J. Hydrogen sulfide attenuates hyperhomocysteinemia-induced

cardiomyocytic endoplasmic reticulum stress in rats. *Antioxid Redox Signal* 12: 1079–1091, 2010.
45. Woo CW, Cui D, Arellano J, Dorweiler B, Harding H, Fitzgerald KA, Ron D, and Tabas I. Adaptive suppression of the ATF4-CHOP branch of the unfolded protein response by toll-like receptor signalling. *Nat Cell Biol* 11: 1473–1480, 2009.
46. Yao LL, Huang XW, Wang YG, Cao YX, Zhang CC, and Zhu YC. Hydrogen sulfide protects cardiomyocytes from hypoxia/reoxygenation-induced apoptosis by preventing GSK-3beta-dependent opening of mPTP. *Am J Physiol Heart Circ Physiol* 298: H1310–H1319, 2010.
47. Yokouchi M, Hiramatsu N, Hayakawa K, Okamura M, Du S, Kasai A, Takano Y, Shitamura A, Shimada T, Yao J, and Kitamura M. Involvement of selective reactive oxygen species upstream of proapoptotic branches of unfolded protein response. *J Biol Chem* 283: 4252–4260, 2008.
48. Zhu J, Rebecchi MJ, Tan M, Glass PS, Brink PR, and Liu L. Age-associated differences in activation of Akt/GSK-3beta signaling pathways and inhibition of mitochondrial permeability transition pore opening in the rat heart. *J Gerontol A Biol Sci Med Sci* 65: 611–619, 2010.

Address correspondence to:
Dr. Jun Ren
Center for Cardiovascular Research and Alternative Medicine
University of Wyoming College of Health Sciences
Laramie, WY 82071

E-mail: jren@uwyo.edu

Date of first submission to ARS Central, November 3, 2010; date of final revised submission, May 5, 2011; date of acceptance, May 5, 2011.

Abbreviations Used

2,4-DNPH = 2, 4-dinitrophenylhydrazine
ATF6 = transcription factor-6
CCCP = carbonyl cyanide m-chlorophenylhydrazone
CM-H2DCFDA = 5-(6)-chloromethyl-2′,7′-dichlorodihydrofluorescein diacetate
+dL/dt = maximal velocities of shortening
–dL/dt = maximal velocities of relengthening
ER = endoplasmic reticulum
FFI = fura-2 fluorescence intensity
GSK3β = glycogen synthase kinase 3β
IRE1 = inositol-requiring protein-1
LVEDD = left ventricular end-diastolic diameter
LVESD = left ventricular end-systolic diameter
mPTP = mitochondrial permeation pore
MTT = 3-(4,5-dimethylthiazol-2-yl)-2,5-diphenyltetrazolium bromide
pAkt = phosphorylated Akt
PEG = polyethylene glycol
PERK = protein kinase RNA-like ER kinase
pGSK3β = phosphorylated GSK3β
PI-3 kinase = phosphatidylinositol 3-kinase
PKR = protein kinase RNA
PS = peak shortening
ROS = reactive oxygen species
TCA = trichloroacetic acid
TN = tunicamycin
TPS = time-to-peak shortening
TR_{90} = time-to-90% relengthening
TUDCA = tauroursodeoxycholic acid
UPR = unfolded protein response
VDAC = voltage-dependent anion channel
WT = wild type

This article has been cited by:

1. Yongxiang Xia, Jianhua Rao, Aihua Yao, Feng Zhang, Guoqiang Li, Xuehao Wang, Ling Lu. 2012. Lithium exacerbates hepatic ischemia/reperfusion injury by inhibiting GSK-3#/NF-#B-mediated protective signaling in mice. *European Journal of Pharmacology* . [CrossRef]
2. Claudia Penna , Maria-Giulia Perrelli , Pasquale Pagliaro . Mitochondrial Pathways, Permeability Transition Pore, and Redox Signaling in Cardioprotection: Therapeutic Implications. *Antioxidants & Redox Signaling*, ahead of print. [Abstract] [Full Text HTML] [Full Text PDF] [Full Text PDF with Links]
3. Y. Zhang, L. Li, Y. Hua, J. M. Nunn, F. Dong, M. Yanagisawa, J. Ren. 2012. Cardiac-specific knockout of ETA receptor mitigates low ambient temperature-induced cardiac hypertrophy and contractile dysfunction. *Journal of Molecular Cell Biology* . [CrossRef]
4. Yingmei Zhang, Sara A Babcock, Nan Hu, Jacalyn R Maris, Haichang Wang, Jun Ren. 2012. Mitochondrial aldehyde dehydrogenase (ALDH2) protects against steptozotocin-induced diabetic cardiomyopathy: role of GSK3beta and mitochondrial function. *BMC Medicine* **10**:1, 40. [CrossRef]
5. Yingmei Zhang, Jun Ren. 2011. Thapsigargin triggers cardiac contractile dysfunction via NADPH oxidase-mediated mitochondrial dysfunction: Role of Akt dephosphorylation. *Free Radical Biology and Medicine* . [CrossRef]